NATIONAL ADVISORY COMMITTEE FOR AERONAUTICS

TECHNICAL NOTE 2974

EXPERIMENTS ON MIXED-FREE- AND -FORCED-CONVECTIVE HEAT TRANSFER CONNECTED WITH TURBULENT FLOW THROUGH A SHORT TUBE

By E. R. G. Eckert, Anthony J. Diaguila, and
Arthur N. Curren

Lewis Flight Propulsion Laboratory
Cleveland, Ohio

Washington
July 1953

NATIONAL ADVISORY COMMITTEE FOR AERONAUTICS

TECHNICAL NOTE 2974

EXPERIMENTS ON MIXED-FREE- AND -FORCED-CONVECTIVE HEAT TRANSFER CONNECTED WITH TURBULENT FLOW THROUGH A SHORT TUBE

By E. R. G. Eckert, Anthony J. Diaguila, and Arthur N. Curren

SUMMARY

Experiments were conducted to obtain information on heat transfer in turbulent, mixed-free- and -forced-convection flow. This flow regime has recently become important in connection with certain engineering applications such as gas turbines and jet engines. The investigation was made in a vertical tube with a length-to-diameter ratio equal to 5. The walls of the tube were heated, and air was conducted through the tube in either an upward or a downward direction. Free convection is created by gravity so that the buoyancy forces in the heated layers near the tube wall were either parallel or opposite to the direction of the forced flow. The Grashof number which characterizes the free-convection effect could be varied between approximately 10^9 and 10^{13} and the Reynolds number characterizing the forced flow varied from 36×10^3 to 377×10^3.

The investigation revealed that the total flow regime as characterized by its Reynolds and Grashof numbers can be subdivided into a forced-flow regime, a free-flow regime, and a mixed-free- and -forced-convection regime. The limits of the different regimes were established in the investigated range, and the local heat-transfer coefficients at the inner surface of the tube were measured.

The knowledge of the limits of the different flow regimes and of the heat transfer in these regimes obtained from the experiments reported herein could be extended by the use of the results of previous investigations into the laminar-flow range, to other length-to-diameter ratios, and to other Prandtl numbers.

INTRODUCTION

Usually in calculations of convective heat-transfer problems, the flow is classified either as forced flow or as free-convection flow. In the former type, the flow is caused by external means such as pumps; whereas, in the latter type, buoyancy forces connected with temperature

differences in the fluid create the flow. Actually, such buoyancy forces are always present in forced-flow heat transfer as well. Usually they are of a smaller order of magnitude than the external forces and may be neglected. In certain engineering applications, however, this cannot be done. It was, for instance, realized quite early that the heat exchange in oil coolers is affected markedly by the free-convection currents superposed to the forced flow. This is caused by the low flow velocities employed in such coolers. More recently, applications have become important in which very large free-convection forces are present. Forced flow through rotating components is always subjected to centrifugal forces and Coriolis forces. In the presence of temperature differences these forces create strong free-convection flows. Cooling of rotating parts in gas turbines and jet engines may be considerably influenced by these conditions. Examples of such applications are cooling of rotating turbine blades and of ram jets in helicopters.

A limited number of experimental investigations have been published and, from these, correlations for mixed-free- and -forced-convection heat transfer have been obtained. Experimental information on heat transfer in flow of oils through tubes to obtain a relation for laminar heat transfer which included the free-convection effect is contained in reference 1. In reference 2 is presented an analysis of laminar mixed-free- and -forced-convection heat transfer in a vertical pipe, and in reference 3 this analysis is compared with experimental information on oil and water. Experiments on flow and heat transfer of water through a cooled vertical pipe ($L/d = 20$) are described in reference 4. (All symbols are defined in appendix A.) The results indicate that experiments were conducted in the transition region between laminar and turbulent flow. In reference 5 measurements on turbulent flow of water through a tube with $L/d = 52$ show a considerable effect of free-convection currents. Calculations on laminar free and mixed flow for different configurations and wall-temperature distributions are presented in references 6 and 7. However, the configurations which are important in engineering applications are numerous. In addition to the geometry of the heat-transferring surfaces, the direction of the forced-flow velocities relative to the free-convection forces and the question of whether the flow is laminar or turbulent are important. Knowledge of even the most common configuration, namely, the flow through a circular tube, is very incomplete. For instance, no investigation is known in which the flow can with certainty be expected to be turbulent. In addition, it will be shown in RESULTS AND DISCUSSION that, even in the flow regions which have been investigated, the recommended correlations are contradictory.

The investigation described in this report was conducted at the NACA Lewis laboratory to obtain information on heat transfer in the mixed-free- and -forced-convection regime for a configuration which previously had not been investigated. The experiment was conducted in a circular tube with forced flow through its interior, with free-convection

forces parallel or opposite to the forced-flow velocities, and with flow in the turbulent range. The apparatus used for this investigation was so designed as to obtain local values of heat-transfer coefficient. The length-to-diameter ratio of the tube was 5. The tube wall was heated by steam to a uniform temperature. The Reynolds number based on the average forced velocity and the tube diameter could be varied between 36×10^3 and 377×10^3. The Grashof number based on the tube length and the temperature difference between the tube wall and the air in the tube varied between 10^9 and 10^{13}.

In addition, a survey is presented of the results of previous investigations and the information obtained from it is combined with the results of the present experiments so as to obtain consistent correlations in a large range of the mixed-flow regime.

APPARATUS

Basic Considerations

The large free-convection forces present in the applications which were mentioned in the introduction cause the Grashof numbers, which characterize the free-convection flow, to become very large (of the order of magnitude of 10^{12}). The influence of free convection on heat transfer is expected to be especially large when the free-convection forces are parallel or opposite to the forced-flow direction. The coolants most widely used are air and water with a Prandtl number between 1 and 10. Although the influence of the Prandtl number is comparatively small, experiments, in order to be useful for these applications, should be conducted with a fluid having a Prandtl number near this range, with very large Grashof numbers, and with the described direction of the body forces. The large Grashof numbers in the applications are caused by large body forces (centrifugal forces and Coriolis forces). Such a force field is complicated by the fact that the acceleration causing the body forces varies locally in direction and magnitude. In experiments designed to obtain basic information, it is desirable to have a simple force field with locally constant acceleration as represented by the gravitational field. In addition, many experimental difficulties are avoided when stationary equipment is used in which the free-convection currents are generated by the gravitational field of the earth. The buoyant forces connected with the gravitational field, however, are much smaller and special attention has to be directed to means by which large Grashof numbers can be obtained. The Grashof number can be increased by increasing the dimensions of the experimental apparatus, by increasing the temperature differences which are imposed on the fluid, or by choosing the proper test fluid. A survey revealed that with a fixed temperature difference approximately the same dimensions of the

test setup are necessary for water and for compressed air with a pressure near 100 pounds per square inch as a test fluid. For most other easily available fluids, an apparatus with larger dimensions must be used to produce the same Grashof numbers. Only the use of liquids near their critical state and of liquid metals would produce the same Grashof numbers in smaller equipment. This possibility, however, was discarded because the Prandtl number of liquid metals and of liquids near their critical state is too far from 1. In addition, such liquids would introduce serious difficulties into the experimentation. It was therefore decided to use compressed air as the test fluid.

The test apparatus then had to consist essentially of a vertical tube of large dimension through which air was conducted in an upward or downward direction. The walls of the tube were heated. Steam was used for this purpose in order to obtain a uniform temprature on the large tube surface.

Tube Arrangement

The apparatus (fig. 1(a)) which was used for the tests to be described was already available in its essential parts from previous investigations on free-convection heat transfer. Various component parts are designated by letters on this figure to simplify references in the text. The apparatus consists essentially of a vertical tube and two covers A. The over-all dimensions of the tube are: height, $13\frac{1}{2}$ feet; outside diameter, 24 inches; and wall thickness, 3/8 inch. The tube was fabricated from mild steel and coated with zinc on the inside and outside surfaces to prevent corrosion. The inside surface was ground smooth after the coating was applied. The height of the remaining roughness along the axial length adjacent to the steam chambers was measured and found not to exceed ± 0.007 inch. This dimension was assumed to be sufficiently small to consider the surface as hydraulically smooth (ref. 8).

Air at approximately 80° F and with pressures from atmospheric to 125 pounds per square inch absolute could be introduced either through the inlet line B_b into the bottom cover or through the inlet line B_t into the top cover. It could also be removed through the exhaust lines C_b, C_t, or D. By proper adjustment of the valves in the air lines, different flow conditions could be produced. Upward flow of the air through the tube was obtained by admitting the air through B_b into the bottom cover. It then had to pass through a dense screen E before it entered the tube proper. It left the tube through another screen E into the top cover and was discharged through the exhaust line C_t. To obtain downward flow in the tube, air was admitted through the line B_t into the top cover, entered the tube through the screen on top of the

tube, left it through the lower screen, and was finally discharged from the bottom cover through the exhaust line C_b. For a study of free-convection heat transfer, air was admitted into the top cover through B_t and removed from the upper portion of the tube through D. In this way cool air was continuously supplied to the upper portion of the tube. Free-convection currents transported the cool air into the heated portions of the tube and replaced the warm-air layer which flowed upward along the heated wall.

The amount of air conducted through the tube was measured by an orifice in the air-supply line. In order to assure that the air entered the tube proper with a constant velocity, the screens E were made very dense. They consisted of a 1/8-inch-thick Fiberglas mat between two 1/4-inch-mesh, 23-gage wire galvanized screens. The screens produced a pressure drop of 5 pounds per square inch at the lowest air flow investigated. Measurements of temperature and velocity profiles in the tube indicated that the screens fulfilled their purpose.

The surface of the tube was heated with low-pressure steam superheated by throttling to 2° or 3° F above the saturation temperature; the pressure ranged from 1 to 3 inches of mercury above atmospheric pressure. Four openings F along the length of the insulated steam jacket G surrounding the tube were used to distribute the steam uniformly throughout the jacket. A steam trap on the main condensate line and a throttle valve on the steam supply line were used to obtain the desired steam pressure.

Sixteen condensate chambers H, $7\frac{1}{2}$ inches wide, were arranged along the length of the heated section of the tube; therefore, only part of the circumference of the tube was covered by them. The chambers varied in length from 6 inches at the top of the tube to $8\frac{1}{2}$ inches at the bottom and trapped only the condensate which developed on the section of the tube wall enclosed by these chambers. From each chamber, 1/2-inch-diameter lines, shown in figure 1(b), carried the condensate through the steam jacket to the condensate measuring apparatus. The exposed portion of these lines (J in fig. 1(a)) was heavily insulated to reduce heat losses.

Condensate Measuring Apparatus

The condensate from the condensate chambers was measured on a burette board (K in fig. 1(a)). Each chamber H was connected to a burette L graduated in tenths of a milliliter. A spherical condensate collector M, $1\frac{3}{4}$ inches in diameter, and a petcock arrangement N at the

top of the burette were necessary because direct connections between the burettes and the lines from the condensate chambers H would permit steam to fill the portion of the burettes not used up by condensate and thus provide an exposed area for steam condensation which would vary with the amount of condensate in the burettes. The burettes were insulated by two layers of air between two Plexiglas windows at the front and an insulating board at the rear. Nevertheless, the condensation caused by the heat losses from the burettes proved inconvenient in the first runs made with direct connections between burettes and condensate lines. The spherical container M, which was installed after this experience, was emptied into the burette as soon as the condensate level had risen to about 1/4 inch above the level indicated in figure 1(a); this provided a relatively large volume of condensate and a small variation in exposed surface area on which steam would condense. The tube, inserted in the container M to slightly below the center, provided a minimum condensate level in the sphere which could be conveniently reproduced. The time required to obtain this amount of condensate ranged from 10 to 30 minutes depending upon the operating conditions and the position of the condensate chambers.

Instrumentation

Five iron-constantan thermocouples O, spaced as shown in figure 1(a), were used to measure the wall temperatures in the heated section. These thermocouples were embedded in holes drilled from the outside into the tube wall to a depth of 1/4 inch. The thermocouple ends were welded into a small copper cylinder which fitted the holes closely. Thermocouple lead wires were attached to the outside wall of the heated tube and brought out of the steam jacket through the bottom flange. Fiberglas insulation and plastic coating protected the thermocouple wires from the steam. Two thermocouples P measured tube-wall temperatures below the heated section.

Steam temperatures were measured by four iron-constantan thermocouples Q spaced along the length of the steam jacket. Each thermocouple was so arranged in a 1/8-inch-diameter tube that the junction was formed by welding the ends into a cap closing the tube. The thermocouple junctions were located midway between the tube wall and the steam-jacket wall.

Air temperatures at various locations along the tube axis were measured with thermocouple probes (fig. 2). The probe locations and identification numbers along the length of the tube are shown by R in figure 1(a). With this arrangement, temperature readings of the heated air in five planes were obtained. Air temperatures were also measured with iron-constantan thermocouples S in the inlet and exhaust lines as indicated on figure 1(a).

The air pressure in the tube was measured with calibrated Bourdon type gages through pressure taps at two locations (T in fig. 1(a)), one near the top and one near the bottom of the tube wall.

Accuracy of Measurements

Calculation of the heat-transfer coefficients on the inside wall of the tube is based on the difference between the air temperature along the axis of the tube and the temperature of the inside-wall surface. Since the wall temperature was measured in the center of the wall, a calculation of the temperature drop due to the heat conduction through the wall was made; it indicated a temperature difference of approximately 1° F. This temperature difference was disregarded. The accuracy of the potentiometer, the calibration accuracy, and the reading accuracy together added up to an error in the wall-temperature measurement of $\pm 2.0^{\circ}$ F. The difference between the temperatures indicated by the thermocouples in the steam jacket and in the wall was between 0.5° and 1° F. Steam temperatures were estimated to be accurate within $\pm 1.5^{\circ}$ F. Readings of the temperature of the heated air at a specified location, however, repeated only within $\pm 3^{\circ}$ to $\pm 5^{\circ}$ F depending on the location of the thermocouples. Fluctuations of the air temperatures seem to be connected with large-scale turbulence which is present in the air, especially under the conditions of counterflow and free-convection flow.

The mercury U-tube measurements of the steam pressure were accurate within ± 0.05 pound per square inch. The saturation temperature determined from this pressure agrees within 1° F with the steam temperature measured by the thermocouples. Air pressures were measured with two Bourdon type gages. The difference between the readings of the gages was small and the average of both was used to determine the air density. The accuracy of these pressure measurements determined by calibration was found to be 2 percent below 30 pounds per square inch absolute and 1 percent above this value. The condensate was collected during the runs and measured volumetrically. Duration of the runs was determined with a stop watch. The measurements of the rate of condensation for the complete run could be reproduced within ± 2.0 percent. The flow orifice for the supply air was calibrated and estimated to be accurate within 1 percent.

CALCULATION OF LOCAL HEAT-TRANSFER COEFFICIENTS

Equation Defining Heat-Transfer Coefficient

The local film heat-transfer coefficients inside the tube at various locations along its length were determined from the following equation:

$$H = \frac{Q_c}{A(t_w - t_a)} \tag{1}$$

In this equation the area A considered for heat transfer was that section of the inside surface of the tube which was enclosed by the individual condensate chamber. Because of the finite thickness of the walls of the condensate chamber, as shown in the detail insert of figure 1(b), two values of the area A can be calculated, one with the inside and one with the outside dimensions. The difference between both areas was less than 1 percent and the mean of the two values was used in the calculation of the heat-transfer coefficient. The temperature of the air t_a in equation (1) was obtained along the tube axis directly opposite the center of the condensate chamber. Figure 3(a) shows the air temperature measured along the tube axis for the free-convection test and figure 3(b), for the mixed-free- and -forced-convection experiments. The air temperatures t_a to be inserted into equation (1) were taken from these figures. The temperature measured in the center of the tube wall was used in equation (1) as the wall temperature t_w. This temperature was constant along the heated section of the tube.

Evaluation of Convective Heat Flow and Heat Loss

Determination of convective heat flow Q_c. - The total heat flow Q which was determined by measurement of the condensate collected in the individual burettes consisted not only of the amount collected in the individual condensate chambers (H in fig. 1(a)) but also of the amounts formed by the heat loss to the surrounding atmosphere from the part of the condensate lines outside the steam jacket (J in fig. 1(a)) and the spherical condensate collectors (M in fig. 1(a)). In addition, heat is transferred from the interior tube surface not only to the air by convection but also to the cooler top and bottom sections by radiation. Correspondingly, the convective heat flow per unit time Q_c may be determined from the equation

$$Q_c = Q - Q_A - Q_R \tag{2}$$

where

$$Q = wh \tag{3}$$

The heat flow to the surrounding atmosphere from the condensate lines and in the spherical collectors is denoted by Q_A and the radiative heat flow, by Q_R in equation (2). In equation (3), the condensate weight flow per unit time is w, the total measured rate for the individual burette corresponding to the condensate chamber (or location along the tube surface) under consideration. The term h is the heat of

vaporization per pound of water at saturation pressure, that is, the measured pressure in the steam jacket. The small degree of superheating was neglected. The heat flow Q obtained by use of equation (3) is therefore the total heat released by condensation of the weight flow w.

Determination of heat loss $Q_A + Q_R$. - In order to determine the convective heat flow Q_c, it is necessary to subtract from the total heat flow Q the heat radiation Q_R and the heat lost to the atmosphere Q_A from the exposed condensate lines and collectors. Both quantities were determined in heat-loss runs. If the tube interior could be completely evacuated, heat would be removed from the interior tube wall only by radiation towards the cooler top and bottom sections. The condensate collected in such a run would be the result of this radiative flow Q_R and the heat losses in the condensate lines and spherical collectors Q_A.

Actually, the laboratory facilities which were connected to this apparatus did not provide complete evacuation of the tube. Therefore, a small convective heat transfer still took place in the interior of the tube, and equation (2) holds for such heat-loss runs as well as for heat-transfer runs. The convective heat flow is, however, much smaller because of the lower density of the air and because the heated air inside the tube is not replaced in these runs but is heated to a temperature near that of the wall. This convective heat flow encountered in heat-loss runs may be indicated by Q_c' and the amount of condensate collected in such a run by w'. Then equation (2) becomes

$$Q_c' = w'h - Q_A - Q_R \tag{4}$$

When the room conditions are the same, the heat lost from the condensate lines and the spherical collectors Q_A is the same as in the actual heat-transfer runs; the radiative heat loss Q_R may be different. However, it will be shown later in this section that this loss is very small. By neglecting the difference in the radiative heat flow occurring during the heat-transfer runs and the heat-loss runs, equations (2) to (4) can be combined

$$Q_c = wh - w'h + Q_c' \tag{5}$$

In this equation w is the amount of condensate collected during a heat-transfer run, w' is the amount collected during a heat-loss run, and Q_c' is the convective heat transfer in a heat-loss run. The value of Q_c' is small compared with the other terms in equation (5) under the test conditions set up in the heat-loss runs and can be determined by the following approximate calculation. Since no information on the specific configuration used for this investigation is available, the calculation

was based on a correlation for a vertical flat plate. The laminar equation was used to obtain the heat-transfer coefficient for the heat-loss runs because the low density of the air in the tube and the small temperature difference lowered the Grashof number for these runs below the critical value. The equation for the average Nusselt number $\overline{Nu}$ in free-convection laminar flow (ref. 9, pp. 522-542) on a vertical plate is

$$\overline{Nu} = 0.555(GrPr)^{\frac{1}{4}} \tag{6}$$

The local Nusselt number which follows was obtained from this relation by multiplying by the factor 3/4 (ref. 10, p. 162):

$$Nu = 0.416(GrPr)^{\frac{1}{4}} \tag{7}$$

With the local heat-transfer coefficient H' determined in this way, the convective heat flow Q_c' was calculated by use of equation (1) and the temperatures t_w and t_a, which were measured during the heat-loss runs. All data were then available to calculate the convective heat flow Q_c in equation (5). The convective heat flow Q_c' encountered during the heat-loss runs amounted to 2 to 4 percent of the convective heat flow Q_c in the heat-transfer runs.

Alternate method of determining heat loss. - A calculation was also made to obtain an estimate of the heat flow by radiation Q_R from the heated walls to the unheated bottom section of the tube. In this calculation, the temperature of the tube surface was assumed to be 212° F and that of the bottom circular surface 90° F. These temperatures are representative of the severest conditions. The emissivity of the galvanized iron surface was taken as 0.20. For the heat-transfer runs, the heat exchange by radiation between the center of the wall section enclosed by the lowest condensate chamber and the bottom plate was calculated on these assumptions to be approximately 0.75 percent of the convective heat flow Q_c. At other locations along the tube wall, the radiative heat transfer was still smaller; therefore, the heat transfer by radiation could be neglected.

The heat loss Q_A in the condensate lines and in the spherical collectors can also be determined by arranging traps at the location where the condensate lines leave the steam jacket. These traps were so designed that no condensate coming from the condensate chambers could flow into the spherical collectors. These collectors then collected only condensate formed on their surfaces and that which formed with the condensate lines

outside the steam jacket. From the condensate measured in the burettes by this method, the heat loss Q_A could be found. The traps were arranged only on a selected number of condensate lines in order to check the heat losses obtained by the first method described. Convective heat flows Q_c determined in this manner agreed with the values obtained by the first method within 3 percent.

Determination of characteristic length x. - For vertical plates, uniformly heated, the characteristic length x, used in the dimensionless parameters Nu, Gr, and Re, is measured from the lower or upstream plate end. In this investigation, however, the wall temperature of the tube was constant only where it was surrounded by the steam jacket (G in fig. 1(a)). Below the steam jacket the wall temperature decreased with distance from the steam jacket. In order to account approximately for this fact, a fictive end of the heated section was established as indicated in figure 4, which applies specifically to a free-convective run. In this figure, the measured wall temperatures are plotted against distance below the end of the steam jacket. The air temperature along the tube axis as extrapolated from the measured values is also indicated on the figure. It can be seen that the temperature difference between the wall and the air decreases with distance below the end of the steam jacket and reaches a value of zero 8 inches below the jacket for this particular run. It can be expected that, for a first approximation, conditions are similar on a tube with a constant temperature difference which has its lower end at a position such that the two dashed areas in figure 4 are equal. In this way, the expression $\int (t_w - t_a)dA$, which is important for the heat transferred, becomes equal for the real tube and the one with a constant temperature difference. The fictive end of the steam jacket was determined in this way. The characteristic length x contained in the Nusselt, Grashof, and Reynolds numbers was measured from the fictive end of the steam jacket to the center of the condensate chamber being considered. Whether this characteristic length is measured from the fictive or the actual end of the steam jacket influences Nusselt and Grashof numbers within the accuracy of the measurements only for the two lower condensate chambers. This will be shown in a later figure.

EXPERIMENTAL PROCEDURE

Heat-loss runs. - The purpose of the heat-loss runs was to determine the values of the two terms $w'h$ and Q_c' in equation (5). In the heat-loss runs, the tube was partially evacuated by reducing the air pressure to 7 inches of mercury absolute, the minimum available to the apparatus from the laboratory altitude-exhaust facilities. Before the data were recorded, the tube was heated by the low-pressure steam for approximately 2 hours. This length of time was required for the tube wall temperatures of the heated and unheated sections and the temperature of the air in the tube to reach equilibrium. After equilibrium was obtained, the quantity of condensate in the burettes was recorded at 20-minute intervals and an

average of at least five readings was obtained. The heat-loss runs were repeated at various intervals throughout the investigation. The heat losses w'h - Q_c' determined in this manner increased from 10 percent of the total heat-flow rate Q at the high-velocity runs to 45 percent for the low-pressure, low-velocity runs.

Heat-transfer runs. - Mixed-free- and -forced-convection heat-transfer runs were made for a series of air pressures inside the tube of approximately 45, 65, and 100 pounds per square inch absolute to obtain high values of Grashof numbers. At each pressure a series of runs was made with forced air flowing in the upward direction with velocities ranging from approximately 1 to 5 feet per second (at the lowest pressure up to 10 ft/sec). The range of velocities was so chosen that they exceed the velocities occurring in a free-convection boundary layer along the tube wall (as calculated in ref. 11). A similar series of runs was made with the forced air flowing in the downward direction. The runs with air flowing in the upward direction are referred to as parallel flow since the forced flow is in the same direction as free-convection flow within the heated boundary layer along the tube wall. The runs in which the forced flow is in the downward direction are referred to as counterflow since the forced flow is in a direction opposite to the flow in a heated free-convection boundary layer along the tube wall. A series of runs was also made in which the air was supplied at the top cover of the tube (line B_t) and discharged through the two exhaust-tube outlets D. No forced flow existed in these runs through the heated portion of the tube, and they were therefore considered as the limiting case of pure free-convection heat transfer. In these runs the air pressure was varied from atmospheric to 125 pounds per square inch absolute, the maximum available pressure.

For each of the heat-transfer runs, the tube was preheated for a period of approximately 2 hours, and data were then taken at 10- to 30-minute intervals. Averages of five to six readings were taken as the final data. Throughout each run, conditions were kept constant. The measurements produced all necessary data for calculating local heat-transfer coefficients. In addition, the temperature and velocity fields of the air inside the tube were investigated by measurement of their profiles along the cylinder radii in the planes indicated in figure 1(a) by the probes R (appendix B).

RESULTS AND DISCUSSION

Present Experiments

Dimensional analysis shows that in the mixed-free- and -forced-convection regime, the average heat-transfer coefficient, when expressed in a dimensionless form as Nusselt number, will depend on the Reynolds

number, the Grashof number, and the Prandtl number for a fluid with constant property values and for geometrically similar configurations. Variable property values would introduce additional parameters; however, in the present investigation the variation of the property values is sufficiently small to neglect the influence of these additional parameters. For flow through tubes, geometric similarity restricts the relation

$$Nu = f(Re, Gr, Pr) \tag{8}$$

to tubes with a certain ratio of length to diameter or, generally, this ratio L/d appears as an additional parameter in the dimensionless relation (8). The local heat-transfer coefficient depends also on the location expressed in dimensionless coordinates. In addition to the described parameters, the heat-transfer coefficient is determined by the boundary conditions, that is, in the present case by the velocity and temperature profile in the entrance cross section and by the variation in temperature over the heat-transfer area.

As described in the previous sections, local heat-transfer coefficients were measured in a vertical tube with a length-to-diameter ratio of 5. The wall temperature was kept constant over the tube surface by heating with steam. Air with a Prandtl number Pr of 0.70 was induced vertically in an upward or downward direction through the tube, and the free-convection forces were generated by the gravitational field of the earth so that the free-convection forces were either parallel or opposite to the forced-flow direction. Special efforts were made to obtain a uniform velocity and temperature profile over the entrance cross section by use of a dense screen.

Parallel flow. - The results of the experiments with the free-convection force parallel to the forced-flow velocity are shown in figure 5. The local Nusselt number Nu_x is plotted against the product Gr_xPr with the Reynolds number Re_d as a parameter. The length parameter used in the Nusselt and Grashof numbers is the distance x from the fictive lower end of the heated tube section to the desired heat-transfer point. The difference between the tube wall temperature t_w and the temperature of the air at the tube axis t_a at the same distance x is used throughout the report to calculate the Grashof number. Physical properties of the air were based on a film temperature $(t_w + t_a)/2$ for all parameters except Re_d, which is based on the temperature of the air averaged along the tube axis. The diameter of the tube and the average velocity of the forced flow were used to obtain the Reynolds number Re_d. The air pressure in the tube, which in turn affects the Grashof and Reynolds number range, could be varied and appears as a parameter for the

different diagrams in the figure. Lines of constant Re_d are drawn through the experimental points. The significance of the points identified as Re_x will be explained later in this section.

As a limiting case, turbulent free-convection flow was investigated in the manner described in the previous section. The results of these runs are shown in figure 6.

Also shown in figure 6 are the Nu_x and Gr_xPr numbers calculated for two points with the effective length x measured from the actual lower end of the steam jacket to the centers of the lower two condensate chambers. These points are connected by arrows with corresponding points calculated by the use of the distance from the fictive end of the steam jacket for the characteristic length. The dashed line in this figure constitutes the mean line through the experimental points.

Inserted in the figure as solid lines are two correlations found in literature for free convection on a vertical plate, one derived from a relation in reference 9 for laminar flow by converting the average heat-transfer coefficient to the local value (eq. (7)) and one obtained theoretically in reference 11. The relation given in reference 11 (eq. (30)) is also for average heat-transfer values and shows that for turbulent flow the heat-transfer coefficient is proportional to the 1/5 power of the distance from the lower plate end. Therefore the local Nusselt number is 1.20 times the average value, and the constant 0.0210 in equation (30) of reference 11 becomes 0.0252 for local heat-transfer values.

The dashed mean data line is, on the average, located 20 percent below the turbulent correlation for the flat plate. Therefore, it can be stated that the experimental points agree quite well with the turbulent flat-plate correlation as might be expected in a tube of small length-to-diameter ratio. In such a tube, the boundary layer which builds up along the wall surface is quite short. Accordingly, the boundary-layer thickness will be small as compared with the tube diameter, and the conditions should be quite similar to those on a flat plate. It is also to be expected that the distance from the starting point of the boundary layer will be the main length parameter on which the flow and the heat transfer depend. Therefore, a diagram in which the Reynolds number based on this distance is used as a parameter should give more information than the presentation in figure 5.

In figure 7 is shown such a diagram which reveals very clearly the transition process between forced- and free-convection flow. To obtain this figure, points of constant Re_x were calculated on the Re_d curves in figure 5 (shown as black points) and transferred into this figure. Averaging lines are drawn through these points. Inserted in the figure as a dashed line is also the free-convection correlation obtained in figure 6. It may be recognized that for large Gr_xPr numbers all constant

Re_x curves converge into this line (free-convection region). On the other hand, each of the lines for constant Reynolds number becomes more and more horizontal with decreasing Gr_xPr numbers, indicating the fact that, for each Reynolds number, the Nusselt number becomes independent of the Gr_xPr numbers in this region (forced-flow regime). Noticeable is a dip on all Re_x curves. Figure 8 shows a cross plot of figure 7 with Nusselt numbers plotted against Reynolds numbers and with the product of Grashof and Prandtl numbers appearing as a parameter. The regions which may be termed pure free and forced convection again may be recognized in this figure by the horizontal trend of the curves towards the lower Reynolds number and by the fact that all the curves tend to converge asymptotically into a single line at the higher Reynolds number. This asymptotic line should be the relation for pure forced-convection flow.

Available correlations for turbulent forced flow are also shown in this figure and the correlation for a turbulent boundary layer along a flat plate (ref. 10, p. 117). The two dashed curves are obtained for two x/d ratios from the following equation:

$$Nu_x = 0.116\left[\left(Re_x\frac{d}{x}\right)^{\frac{2}{3}} - 125\right](Pr)^{\frac{1}{3}}\left(\frac{x}{d}\right)\left[1 + \frac{1}{3}\left(\frac{d}{x}\right)^{\frac{2}{3}}\right] \qquad (9)$$

This equation is derived in appendix C from an empirical relation for the average heat transfer determined by Hausen (ref. 10, p. 115) from experiments in the entrance region of a circular tube by again converting the equation to the local values. The curve for the smaller x/d ratio agrees quite well with the relation for a flat plate, as would be expected. The values given by the curve for $x/d = 5$, however, are already higher than the flat-plate values, indicating the fact that the development of the boundary layer in a tube is already different from the one on a flat plate for this length-to-diameter ratio. The length-to-diameter ratio increases along the curves of constant Gr_xPr from left to right, ending with the ratio $x/d = 5$. Therefore, it can be stated that the agreement between the measured heat-transfer coefficients in the forced-flow region and the values predicted by Hausen's relation is satisfactory. Even the dip in the curves of constant Gr_xPr is explained by the fact that the x/d ratio along the curves increases from smaller to larger values towards the right.

Of primary interest for the investigated problem is the question in which range of Reynolds and Grashof numbers the heat transfer may be considered as pure forced convective, as pure free convective, or as mixed forced and free convective. The determination of the limits between these regimes requires some arbitrary definition since actually the transition of the mixed-flow region into the other two regimes is asymptotic.

The forced-flow regime will be defined as that part in which the influence of the Grashof number changes the heat-transfer coefficient by not more than 10 percent. A corresponding definition will be applied to the limit of the free-convective regime. The limiting lines were determined in this way from figure 7 and are transferred into a Reynolds-Grashof diagram as presented in figure 9. The two highest curves represent these limits. The lowest curve will be discussed in the section Counterflow.

The free-convection line was determined in figure 7 by finding the values Gr_xPr for which the Nusselt numbers determined by the lines Re_x = constant have values 10 percent above the dashed line representing the free-convection heat transfer. The forced-convection limit was determined from the curve shown in figure 7. This diagram (fig. 9) may be used to determine in any special case whether the heat-transfer coefficients should be calculated from forced-flow equations or from free-convection equations, or whether they will be in the transition regime. It can be seen that the Grashof-Prandtl numbers appearing in this diagram are above the critical value 10^8 for transition to turbulence. The Reynolds numbers are partially above, partially close to the limit. From information on flat plates, this value is expected to be of the order of 10^5. Therefore, it should be safe to assume that the flow is turbulent in the whole field covered by figure 9. The limiting line between the free- and mixed-flow regimes can be expressed as

$$Re_x = 8.25(Gr_xPr)^{0.40} \tag{10}$$

and the limiting line between the forced- and mixed-flow regimes as

$$Re_x = 15.0(Gr_xPr)^{0.40} \tag{11}$$

McAdams (ref. 12, p. 207) proposed the following rule: In cases in which it is doubtful whether forced- or free-convection flow applies, the heat-transfer coefficient should be calculated using both the forced- and the free-convective relations, and the larger one should be used. An investigation of figure 7 shows that in the mixed-flow regime the actual heat-transfer coefficients are always somewhat smaller than the one determined by this rule, the largest deviation being approximately 25 percent, so that the rule by McAdams gives correct values within this degree of accuracy.

Counterflow. - The results of the runs in which the forced flow was in a downward direction are shown in figure 10. In these runs, therefore, the direction of the free-convection forces was opposite to the direction of the mean forced velocity. The presentation is the same as in figure 5. The use of the Reynolds number based on the distance x from the fictive lower end of the heated section converts figure 10 into figure 11. Also inserted in figure 11 is a dashed line which averages the results of the experiments with pure free-convection flow (fig. 6).

It may be observed that the curves with constant Reynolds number Re_x again converge for large Grashof numbers asymptotically toward the free-convection mean data line from figure 6. However, the approach appears to be more gradual in this case than in the case of parallel flow. The limit of the free-convection regime can again be found as a line located 10 percent above the line into which the curves for constant Re_x converge. This limiting line between free and mixed flow, shown in figure 9, is expressed by the equation

$$Re_x = 18.15(Gr_xPr)^{0.33} \qquad (12)$$

In determining the corresponding limit for pure forced flow, however, the following difficulty is encountered: For pure forced flow in a downward direction it has to be expected that the boundary layers which determine the heat transfer start at the upper end of the heated tube section and increase in thickness in the downward direction. Accordingly, the length parameter which mainly determines the magnitude of the heat-transfer coefficient is expected to be the distance from the upper end of the heated section. In figure 11, however, all the parameters are based on the distance from the lower end of the heated section. Another figure was therefore prepared in which all the parameters were converted to the ones which use the distance ξ measured from the upper end of the heated section as the characteristic length. For this purpose the experimental points shown in figure 10 were recalculated to determine the relation in the new parameters. Averaging curves of Re_ξ were inserted in a plot of Nu_ξ against $Gr_\xi Pr$, which contained these points. The other steps in the procedure were identical to the ones leading from figure 5 to figure 8. Figure 12 shows the result with the Reynolds number Re_ξ as the abscissa and the product of Grashof number Gr_ξ and Prandtl number Pr as a parameter. Again the curves for pure forced flow, which were already presented in figure 8, are inserted as dashed lines. It is indicated that the curves of constant Grashof number have the tendency to approach these lines asymptotically; however, in the investigated range they are still a considerable distance away from the forced-convection limits. Accordingly, it can be concluded that the mixed-flow regime approaches the pure forced-flow conditions much more gradually for counterflow than for parallel flow. The velocity range of the investigation was not sufficient to determine the 10-percent limit between the mixed- and the forced-flow regimes. The available facilities prevented a further increase in the forced-flow velocities.

A plot analogous to figure 12 but with all parameters based on the distance x from the downward end was also prepared. As expected, convergence of the Gr_xPr curves towards the forced-flow relations was not as readily apparent as when the curves were based on the distance ξ.

In accordance with this more gradual transition from free to forced convection, the heat-transfer coefficients found in the counterflow experiments are up to two times larger than the higher of the values calculated for pure forced- or free-convection flow. This is astonishing since it might be expected that the free- and forced-convection forces acting in opposite directions tend to cancel each other partially and in this way reduce the heat-transfer coefficients to values even below the pure free- or forced-flow conditions. The cause for the large heat-transfer coefficients which were actually found probably results from an increased turbulence which is very likely under the condition in which the flow in the central core of the tube tends to move in a direction opposite to the flow in the heated boundary layers near the wall. This movement in different directions may be recognized from some of the velocity profiles presented in appendix B.

Experiments by Watzinger and Johnson

In reference 4 the results of an experimental investigation on a vertical tube with a ratio $L/d = 20$ are presented. The entrance conditions were again uniform with respect to temperature and velocity. Warm water was directed in a downward direction through the tube which had externally cooled walls. Therefore, in the investigation the free-convection forces were parallel to the direction of the forced-flow velocities. The Prandtl number based on the film temperature varied within the limits of 2 to 5. The reference report lists the value (table III) of the average Nusselt numbers Nu_d as well as the Reynolds Re_d and Grashof numbers Gr_d. The length used in all the parameters was the diameter d of the tube. It appears reasonable to expect that for the comparatively large length-to-diameter ratio, heat transfer should be mainly determined by this length parameter.

Figures 13 and 14 were obtained from the data in reference 4. They reveal essentially the same features as figures 7 and 8, in which at high values of Re_d and Gr_d the results converge on available correlations for turbulent-forced-flow and for turbulent-free-flow heat transfer. A dip can be observed this time in both the Re_d = constant curves in figure 13 and in the Gr_d = constant curves in figure 14. It may be connected with the transition process to turbulence. The difference that in the present tests the dip occurs only on the curves of Re_x = constant (fig. 7) would then be explainable by the fact that transition starts in different regions of the Re-Gr field. Again the limits between the different flow regimes were determined in figures 13 and 14 and are shown in figure 15. The limiting line between the free- and the mixed-flow regime can be presented by

$$Re_d = 7.39(Gr_d)^{0.35} \tag{13}$$

and the one between the forced and the mixed-flow regime by

and the one between the forced and the mixed-flow regime by

$$Re_d = 19.64(Gr_d)^{0.35} \tag{14}$$

A few experiments were done in the same apparatus also under the condition of counterflow. Watzinger and Johnson compared the heat transfer obtained in counterflow with that obtained for parallel flow in a figure in which the heat-transfer coefficients are plotted as functions of the temperature difference between the tube wall and the fluid. The counterflow heat-transfer coefficients were found to be larger in the entire investigated range. The differences between both values were between 6 and 20 percent, with the largest difference found at high Reynolds and Grashof numbers. This fact is in qualitative agreement with the results of the investigation presented in this report.

The tests seem to have covered the transition region between laminar and turbulent flow. Correspondingly, Watzinger and Johnson used a laminar correlation as a limiting free-flow condition (fig. 13). Obviously, the turbulent correlation inserted in figures 13 and 14 is the one towards which the curves of Re_d and Gr_d = constant tend asymptotically.

Results Obtained by Martinelli and Boelter

In reference 2 is presented a theory by which heat transfer in a tube for the mixed regime of free and forced convection under the condition of laminar flow could be calculated. For the calculation it was assumed that the free-convection forces are parallel to the forced-flow velocities and that the heat transfer is primarily determined by the conditions near the tube wall. Accordingly, the velocity profile in the flow was approximated by a linear velocity increase with distance from the wall. The density was assumed to be a linear function of temperature. In one step, which is called the second approximation in reference 2, the temperature in the bulk of the fluid was assumed constant and equal to the entrance temperature, thus restricing this analysis to short tubes. The following equation for the average Nusselt number in a tube of length L was obtained:

$$\overline{Nu}_d = 1.75 \sqrt[3]{Gz_d + 0.0722\left(Gr_d Pr \frac{d}{L}\right)^{0.75}} \tag{15}$$

This equation is also applicable for forced flow by neglecting the second term and for free flow by omitting the first term. The Graetz number Gz is connected with the Reynolds and Prandtl numbers by the following relation:

A third approximation took into account the temperature increase which occurs in the bulk of the fluid in tubes of larger L/d ratio. The result of this calculation differs from equation (15) only in the way that the two numerical constants 1.75 and 0.0722 are replaced by two functions of the ratio Nu/Gz. These functions are tabulated in reference 2. In a later paper (ref. 3) it is proposed to change the exponent on the parameter which contains the Grashof number from 0.75 to 0.84 in order to obtain better agreement with the experimental results contained in the same paper. This change is justified by the assumption that some turbulence was present in the experimental apparatus. In this report equation (15) will be used to obtain information for the laminar region and, therefore, the exponent 0.75 is retained.

The average heat-transfer coefficient which is contained in the Nusselt number expressed by equation (15) is based on the arithmetic mean between the temperature difference in the entrance and exit cross section. Norris and Streid (ref. 13) pointed out the fact that it is more advantageous to base the heat-transfer coefficient on the logarithmic mean of entrance and exit temperature differences because the Nusselt number calculated in this way approaches a constant value for small Graetz numbers (for large L/d) which is identical with the Nusselt number in the region of fully developed flow. Figure 16 is a plot of the average Nusselt numbers as calculated by Martinelli and Boelter (ref. 2) with the change that the Nusselt numbers are based on the logarithmic mean temperature difference. Inserted in the figure are also the heat-transfer coefficients obtained by the second approximation in reference 2 and the correlation for pure-free-convection heat transfer recommended in reference 13. The lines in this figure, which present the third approximation, exhibit, at low values of the Graetz number, the following physically improbable features: They start at a certain limit to increase with decreasing Graetz number and to go asymptotically toward infinity. The lines for the two lowest values of the parameter $Gr_d Pr \frac{d}{L}$ reach values of the Nusselt number which are below the pure-free-convection correlation. It is therefore believed that the validity of the calculated curve is restricted to the range in which they are shown as solid lines, and it is doubtful whether in this range the third approximation is a better solution than the second one.

Accepting equation (15) for the heat-transfer coefficients in short tubes for laminar-flow conditions gives the possibility to calculate again the two limits for which the mixed-flow heat-transfer coefficients exceed the heat-transfer coefficients for pure forced flow or pure free flow, respectively, by 10 percent. The following equations describe these limits:

$$\text{Forced-flow limit:}\quad Gz_d = 0.217\left(Gr_d Pr\,\frac{d}{L}\right)^{0.75} \tag{17}$$

$$\text{Free-flow limit:}\quad Gz_d = 0.0241\left(Gr_d Pr\,\frac{d}{L}\right)^{0.75} \tag{18}$$

Expressed in Reynolds numbers instead of Graetz numbers, the limits become

$$\text{Forced-flow limit:}\quad Re_d Pr\,\frac{d}{L} = 0.276\left(Gr_d Pr\,\frac{d}{L}\right)^{0.75} \tag{19}$$

$$\text{Free-flow limit:}\quad Re_d Pr\,\frac{d}{L} = 0.0307\left(Gr_d Pr\,\frac{d}{L}\right)^{0.75} \tag{20}$$

Figure 17 presents again the forced-flow regime, the mixed-flow regime, and the free-convection regime in the Grashof-Reynolds field.

By combining all the available information it is possible to obtain a tentative survey over the different regimes in the entire range of Reynolds and Grashof numbers for a tube with parallel flow. Such a survey is presented in figure 18. For Reynolds and Grashof numbers, which are expected to characterize laminar-flow conditions, equations (19) and (20) were used to determine the limits between the different flow regimes. The limits are calculated for two L/d ratios (5 and 20) and for two values of the Prandtl number (0.7 and 3). It can be concluded that the limits between the different flow regimes are, at least in the laminar range, not greatly affected by a change in either parameter. Information on the limits in the turbulent-flow regime can be obtained from the present experimental results. However, the following difficulty arises in this connection: The experiments described in this report determined the limits for the local heat-transfer coefficients, whereas all the previous information was concerned only with average heat-transfer values. In order to be able to introduce the limits for the turbulent range into figure 18, it was assumed that the local conditions at the exit cross section ($x = L$) are identical with the conditions for the average heat transfer in the tube length L. The parameters Re_x and Gr_x in equations (10), (11), and (12) were converted to the ones used in figure 18, and the limits were inserted in this figure. In order to get information on the position of the different regimes in the transitional region between laminar and turbulent flow, the limits obtained in Watzinger and Johnsen's investigation (ref. 4) have also been inserted into figure 18. Of course, it has to be kept in mind that these limits were obtained for tubes with a different L/d ratio (20) and with a different Prandtl number (approximately 3) from the limits in the turbulent regime.

For counterflow conditions only one limit has been determined up to now, namely, the free-convection limit shown in figure 9. In addition, it is known only that the mixed-flow regime extends farther into the forced-flow region for counterflow than for parallel flow. Generally speaking, it may be expected that the location of the mixed-flow regime in the Gr-Re plot is approximately the same for counterflow as for parallel flow but that the width of the mixed-flow regime is larger for the first flow condition.

Comparison with Other Correlations

Colburn offered, in reference 1, the following correlation for heat transfer in the mixed-flow regime

$$\overline{Nu}_d = 1.65(Gz_d)^{\frac{1}{3}}\left(\frac{\mu_w}{\mu_f}\right)^{\frac{1}{3}}\left[1 + 0.015(Gr_d)^{\frac{1}{3}}\right] \tag{21}$$

In this equation μ_w is the viscosity at the wall temperature and μ_f, at the film temperature; the ratio accounts for the dependence of the heat-transfer coefficient on the variation of the property values. The equation was obtained from experimental information available at the time reference 1 was written. The limit for which the mixed-flow Nusselt number exceeds the pure-free-flow value by 10 percent is found from this equation as $Gr_d = 300$. It is independent of the Graetz or Reynolds number. This value would give a vertical line in figure 18 and does not, therefore, agree with the other correlations. The reason for this fact is probably the small amount of experimental information available at the time when reference 1 was published.

It has been mentioned in the section Parallel Flow that McAdams' rule offered in reference 12 agrees within 25 percent with the findings of this report with respect to the values of the heat-transfer coefficients. Experiments with water flowing through a vertical tube with an L/d ratio of 126, a Reynolds number range from 500 to 2700, and with a Grashof number near 10^7 made by E. B. Weinberg are contained in reference 3. The Nusselt numbers agree on an average with the results of reference 4. There exists, however, a wider spread of the individual Nusselt numbers without a clear influence of the Reynolds number on these values. Measurements by E. B. Weinberg, G. Alves, and C. J. Southwell, also contained in reference 3, were made with oil flowing through a tube with a length-to-diameter ratio of 300 and 600, with Grashof numbers near 10^5, and with a Reynolds number range from 1 to 2300. The flow for these conditions should be in the laminar range; however, the L/d ratio is too large for a comparison with the calculations in reference 2, and the limited range of Grashof numbers prevented a presentation of the data in a form analogous to the results of this investigation.

An extensive theoretical investigation on mixed heat transfer in tubes is contained in reference 6. This reference deals, however, only with laminar-flow conditions and with boundary conditions which are quite different from the ones considered here. An interesting analysis for laminar-free-convection heat transfer in a vertical duct is contained in reference 7. It is pointed out that in cases where the free-convection forces are large, the heat transfer may be influenced considerably by internal frictional heating. In the presently discussed experiments, this factor can be neglected. Significant effects of free convection on heat transfer from the walls of a vertical tube to water flowing in an upward direction through the tube are presented in reference 5. No quantitative check with the results reported herein is possible, however, since the published data are not sufficient to calculate the Grashof numbers. The length-to-diameter ratio of the tube used in these experiments was 52.

RESULTS AND CONCLUSIONS

Local heat-transfer coefficients in turbulent flow were measured in a tube with a length-to-diameter ratio of 5 and with free-convection forces which were either parallel or opposite to the forced-flow velocities. The experiments were made with air (Prandtl number, Pr, 0.70). The results of these investigations were supplemented by the results of previous investigations and led to the following conclusions:

1. The whole range of Reynolds Re_x and Grashof Gr_x numbers can be subdivided into a forced-flow regime, a mixed-flow regime, and a free-flow regime in the case of parallel flow. The limit between the free-flow regime and the mixed-flow regime is given in the turbulent-flow range for a length-to-diameter ratio of 5 and a Prandtl number of 0.70 by the following equation:

$$Re_x = 8.25(Gr_x Pr)^{0.40} \tag{10}$$

The corresponding limit between the mixed-flow regime and the forced-flow regime is

$$Re_x = 15.0(Gr_x Pr)^{0.40} \tag{11}$$

The heat transfer in the forced- and in the free-flow regime may be calculated by available relations. In the mixed-flow regime the heat-transfer coefficient deviates up to 25 percent from the larger of the two coefficients calculated with forced-flow and with free-convection relations.

2. The same flow regimes exist in the case of counterflow. The limit equation between the free-flow and the mixed-flow regime in the turbulent-flow range for a length-to-diameter ratio of 5 and a Prandtl number of 0.70 is

$$Re_x = 18.15(Gr_x Pr)^{0.33} \tag{12}$$

The corresponding limit between forced- and mixed-flow regimes was outside the range of the present experiments and could not be determined. The heat-transfer coefficients in the forced- and free-flow regime can again be calculated by available correlations. In the mixed-flow regime the heat-transfer coefficients are always larger than the larger of the calculated forced-flow or free-flow heat-transfer coefficients. The measured value was found to be, at the maximum, approximately twice as large as the calculated value.

3. Information on the different flow regimes in the transition region between laminar and turbulent flow was obtained from experiments by Watzinger and Johnson (ref. 4). The limit equation, expressed by the Reynolds Re_d and Grashof Gr_d numbers, between free and mixed flow in tubes with a length-to-diameter ratio of 20 and a Prandtl number of approximately 3 is

$$Re_d = 7.39(Gr_d)^{0.35} \tag{13}$$

and the limit equation between forced flow and mixed flow is

$$Re_d = 19.64(Gr_d)^{0.35} \tag{14}$$

The equations hold for free-convection forces parallel to the forced flow. In the forced-flow regime and the free-flow regimes, the heat-transfer coefficient could be calculated from available correlations for heat transfer. For counterflow, somewhat higher heat-transfer coefficients were obtained in the mixed-flow regime than for parallel flow.

4. In the laminar-flow range for short tubes and parallel flow, the limits between the different flow regimes were obtained utilizing a theoretical development by Martinelli and Boelter. The limit equation, expressed by the Graetz Gz_d, Grashof Gr_d, and Prandtl Pr numbers, between forced flow and mixed flow is

$$Gz_d = 0.217\left(Gr_d Pr\,\frac{d}{L}\right)^{0.75} \tag{17}$$

The free-flow limit is

$$Gz_d = 0.0241 \left(Gr_d Pr \frac{d}{L} \right)^{0.75} \tag{18}$$

Heat-transfer coefficients in the mixed-flow regime may be determined by calculating the Nusselt number $\overline{Nu}_d$ from the relation

$$\overline{Nu}_d = 1.75 \sqrt[3]{Gz_d + 0.0722 \left(Gr_d Pr \frac{d}{L} \right)^{0.75}} \tag{15}$$

For forced flow the second term in the relation may be neglected and for free flow the first term may be omitted.

Lewis Flight Propulsion Laboratory
National Advisory Committee for Aeronautics
Cleveland, Ohio, April 3, 1953

APPENDIX A

SYMBOLS

The following symbols are used in this report:

A	inside area of section of tube surrounded by condensate chamber, sq ft
C	constant
c_p	specific heat of fluid at constant pressure, Btu/(lb)($^{\circ}$F)
d	inside diameter of tube, ft
Gr	Grashof number, $x^3\beta g(t_w - t_a)/\nu^2$, $d^3\beta g(t_w - t_a)/\nu^2$, or $\xi^3\beta g(t_w - t_a)/\nu^2$
Gz	Graetz number $\left(\frac{\pi}{4}\,\mathrm{RePr}\,\frac{d}{L}\right)$
g	acceleration due to gravity, 32.2 ft/sec^2
H	local heat-transfer coefficient, Btu/($^{\circ}$F)(sq ft)(sec)
h	heat of vaporization of water, Btu/lb
k	thermal conductivity of fluid, Btu/($^{\circ}$F)(ft)(sec)
L	length, ft
Nu	local Nusselt number, Hx/k, Hd/k, or Hξ/k
Pr	Prandtl number, $c_p\mu/k$
Q	heat flow, Btu/sec
Re	Reynolds number, $\rho vx/\mu$, $\rho vd/\mu$, or $\rho v\xi/\mu$
t	temperature, $^{\circ}$F
v	average velocity, $4W/\pi\rho d^2$
W	forced air flow, lb/sec
w	condensate weight flow, lb/sec

x characteristic dimension measured from lower heated edge, ft

β coefficient of thermal expansion of fluid, $1/^{\circ}R$

μ dynamic viscosity of fluid, lb/(sec)(ft)

ν kinematic viscosity of fluid, μ/ρ, sq ft/sec

ξ characteristic dimension measured downward from upper heated edge, ft

ρ density of fluid, lb/cu ft

Subscripts:

A atmosphere

a air

B bulk

c convective

d based on diameter

f film

R radiation

w wall

x based on dimension x

ξ based on dimension ξ

Superscripts:

' value obtained in heat-loss runs

$-$ average

APPENDIX B

TEMPERATURE AND VELOCITY PROFILES

For some of the test conditions the temperature and velocity profiles along the tube radii were measured in several planes normal to the tube axis. The measurements were made with a hot-wire instrument shown in figure 19, which was used alternately as a resistance thermometer and as a hot-wire anemometer. The probe was inserted on the same planes on which the measurement of the air temperature in the tube axis with the thermocouple probes was made. The probe locations and identification numbers along the length of the tube are those shown by R in figure 1(a). The probes transversed from the center of the tube to the tube wall adjacent to the condensate chambers by means of a motor-driving arrangement on the probe mounting. In some tests the profiles were measured over the whole diameter and satisfactory symmetry about the tube axis was observed. A bridge, a galvanometer, and a battery circuit which measure the change of resistance with temperature of the 0.0004-inch-diameter nickel wire are used in connection with the hot-wire instrument.

Temperature Profiles

The air-temperature profiles obtained with the hot-wire instrument are presented in figure 20 for parallel forced- and free-convection flow with two different average forced-flow velocities. The results of the measurements for counterflow with two velocities are presented in figure 21 and for free-convection flow alone, in figure 22. The shape of the temperature profiles is quite similar to the shape of a temperature profile in forced turbulent flow. This is especially true for the parallel-flow condition for which the comparison may be carried somewhat further. On a semilogarithmic plot, most of the measured profiles can be quite well approximated by straight lines. Such a straight-line relation has been established for velocity and temperature profiles in turbulent forced flow of air. The temperature increase with increasing wall distance, however, is smaller than for forced flow. A comparison of the distance from the heated wall to which the temperature change is confined with the corresponding boundary-layer thickness for free-convection flow and forced flow on a vertical plate seemed desirable. Therefore, the boundary-layer thickness for a turbulent free-convection boundary layer on a vertical plate was calculated by the relations contained in reference 11, and the outer limit of the boundary layer is indicated by the diamond symbol in figures 20 to 22. The same calculation was made from an equation for turbulent forced-flow boundary layer as given in reference 10 (p. 75). The result of this calculation is shown by a square in figures 20 and 21. The thickness of the mixed-flow boundary layers agrees reasonably with the calculated ones for parallel flow and free-convection flow.

For counterflow, the temperature gradients extend considerably farther away from the wall than the indicated limits of the free or forced boundary layer. This is interpreted as an indication that intense turbulence with a correspondingly large heat transport is present under counterflow conditions.

Velocity Profiles

The attempt to measure the velocity profiles was not too successful. Unfortunately it was not possible to calibrate the hot-wire anemometer at the air pressures which were used in the apparatus. This may account for the fact that the average air velocities, as obtained with the hot-wire anemometer, differed in some cases by up to 100 percent from the average air velocities as they were calculated from the orifice readings in the intake lines. It may also be that the turbulent fluctuations present in the air cause the anemometer to indicate an apparent velocity which is larger than the actual time-mean velocity in the direction of the tube axis. The velocity profiles which were obtained with the anemometer can, therefore, be considered only as qualitative information. They are presented in figure 23 for parallel flow and counterflow. The shape of the profiles agrees with what would be expected for the corresponding flow conditions. The velocity drop to the value zero near the wall is confined to such a small region that it could not be detected in most of the measurements. Actual counterflow with different directions of the flow velocity near the wall and in the core of the fluid could be observed only in figure 23(c). At the large forced-flow velocity shown in figure 23(d), the free-convection forces were obviously not sufficient to generate a flow in the upward direction even near the wall. It should be pointed out that some uncertainty in the interpretation of the measurements exists in this connection since the hot-wire anemometer gives no indication of the direction of the flow.

APPENDIX C

INTAKE-REGION HEAT-TRANSFER COEFFICIENTS

The following expression was determined by Hausen from available results of experimental investigations for the average heat-transfer coefficient connected with turbulent flow in the intake region of a tube (see ref. 10, p. 115):

$$\overline{Nu}_d = 0.116\left[(Re_d)^{\frac{2}{3}} - 125\right](Pr)^{\frac{1}{3}}\left[1 + \left(\frac{d}{x}\right)^{\frac{2}{3}}\right]\left(\frac{\mu_B}{\mu_W}\right)^{0.14} \tag{C1}$$

The last term in this equation accounts for a variation of viscosity with temperature. This term will be set equal to 1 since the viscosity variation in the experiments reported herein was very small. The average Nusselt number $\overline{Nu}$ contained in this relation can be converted to the local value Nu by the following method: The heat flow Q transferred to the wall of the tube inlet section of length x is equal to the average heat-transfer coefficient $\overline{H}$ multiplied by the circumference $d\pi$, the length x, and the difference between wall temperature and air bulk temperature

$$Q = d\pi(t_w - t_a)\overline{H}x \tag{C2}$$

The air bulk temperature stays practically constant and equal to the air temperature at the tube axis, especially in the region near the entrance. Therefore, the heat flow can be expressed also by the local heat-transfer coefficient H with the equation

$$Q = d\pi(t_w - t_a)\int_0^x H\,dx \tag{C3}$$

Combining equations (C2) and (C3) gives

$$\overline{H}x = \int_0^x H\,dx \tag{C4}$$

Differentiating equation (C4) results in

$$H = \frac{d(\overline{H}x)}{dx} \tag{C5}$$

Equation (C1) can be written in the following way when the terms which do not depend on x are combined in a constant C:

$$\overline{H} = C\left[1 + \left(\frac{d}{x}\right)^{\frac{2}{3}}\right] \tag{C6}$$

Inserting this expression into equation (C5) and performing the differentiation lead to

$$H = C\left[1 + \frac{1}{3}\left(\frac{d}{x}\right)^{\frac{2}{3}}\right] \tag{C7}$$

A replacement of the constant C by the original parameters finally results in the following equation for the local Nusselt number $Nu_x = \frac{Hx}{k}$

$$Nu_x = 0.116\left[\left(Re_x \frac{d}{x}\right)^{\frac{2}{3}} - 125\right](Pr)^{\frac{1}{3}}\left(\frac{x}{d}\right)\left[1 + \frac{1}{3}\left(\frac{d}{x}\right)^{\frac{2}{3}}\right] \tag{C8 or 9}$$

The accuracy of this equation should not be overestimated since the inaccuracy contained in the relation (C1) is accentuated by the differentiation process. Nevertheless it should be useful for the purpose of the present report.

REFERENCES

1. Colburn, Allan P.: A Method of Correlating Forced Convection Heat Transfer Data and a Comparison with Fluid Friction. Am. Inst. Chem. Eng. Trans., vol. XXIX, 1933, pp. 174-210.

2. Martinelli, R. C., and Boelter, L. M. K.: The Analytical Prediction of Superposed Free and Forced Viscous Convection in a Vertical Pipe. Univ. Calif. Press (Berkeley and Los Angeles), 1942.

3. Martinelli, R. C., Southwell, C. J., Alves, G., Craig, H. L., Weinberg, E. B., Lansing, N. F., and Boelter, L. M. K.: Heat Transfer and Pressure Drop for a Fluid Flowing in the Viscous Region Through a Vertical Pipe. Part 1. - Heat Transfer Data. Am. Inst. Chem. Eng. Trans., vol. 38, no. 3, 1942, pp. 493-530.

4. Watzinger, A., und Johnson Dag G.: Wärmeübertragung von Wasser an Rohrwand bei senkrechter Strömung in Übergangsgebiet zwischen laminarer und turbulenter Strömung. Forsch. Geb. Ing.-Wes., Bd. 10, Heft 4, Juli/Aug. 1939, pp. 182-196.

5. Clark, John A., and Rohsenow, Warren M.: Local Boiling Heat Transfer to Water at Low Reynolds Numbers and High Pressure. Div. Ind. Cooperation, M.I.T., July 1, 1952. (For Office Naval Res., Contract N5ori-07827; NR-035-267; D.I.C. Proj. No. 6627.)

6. Ostroumov, G. A.: Mathematical Theory of the Steady Heat Transfer in a Circular Vertical Hole with Superposition of Forced and Free Laminar Convection. Jour. Tech. Phys., vol. XX, no. 6, 1950.

7. Ostrach, Simon: Laminar Natural-Convection Flow and Heat Transfer of Fluids with and without Heat Sources in Channels with Constant Wall Temperatures. NACA TN 2863, 1952.

8. Schlichting, H.: Lecture Series "Boundary Layer Theory." Part II - Turbulent Flows. NACA TM 1218, 1949.

9. Jakob, Max: Heat Transfer. Vol. I. John Wiley & Sons, Inc., 1949, pp. 522-542.

10. Eckert, E. R. G.: Introduction to the Transfer of Heat and Mass. McGraw-Hill Book Co., Inc., 1950.

11. Eckert, E. R. G., and Jackson, Thomas W.: Analysis of Turbulent Free-Convection Boundary Layer on Flat Plate. NACA Rep. 1015, 1951. (Supersedes NACA TN 2207.)

12. McAdams, William H.: Heat Transmission. Second ed., McGraw-Hill Book Co., Inc., 1942.

13. Norris, R. H., and Streid, D. D.: Laminar-Flow Heat-Transfer Coefficients for Ducts. A.S.M.E. Trans., vol. 62, no. 6, Aug. 1940, pp. 525-533.

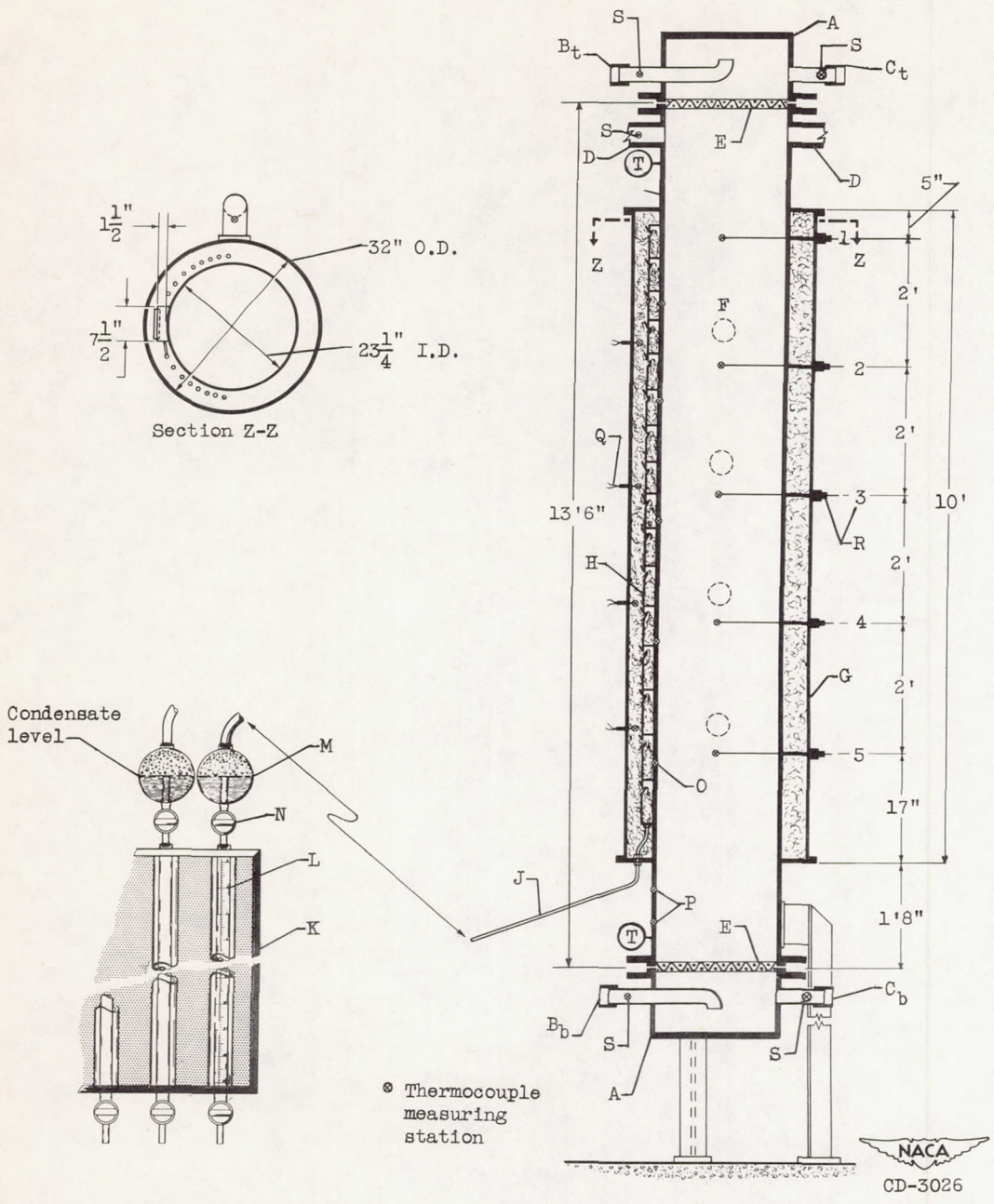

A	Top and bottom covers	F	Inlets to steam jacket	O	Heated-wall thermocouple
B_b	Inlet-line bottom cover	G	Steam jacket	P	Unheated-wall thermocouple
B_t	Inlet-line top cover	H	Condensate chambers	Q	Steam thermocouple
C_b	Exhaust-line bottom cover	J	Condensate lines (exposed)	R	Probes
C_t	Exhaust-line top cover	K	Burette board	S	Inlet- and exhaust-air thermocouples
D	Exhaust line on tube	L	Burette	T	Air pressure taps
E	Screening	M	Condensate collector		
		N	Petcock		

(a) Apparatus.

Figure 1. - Mixed-free- and -forced-convection tube.

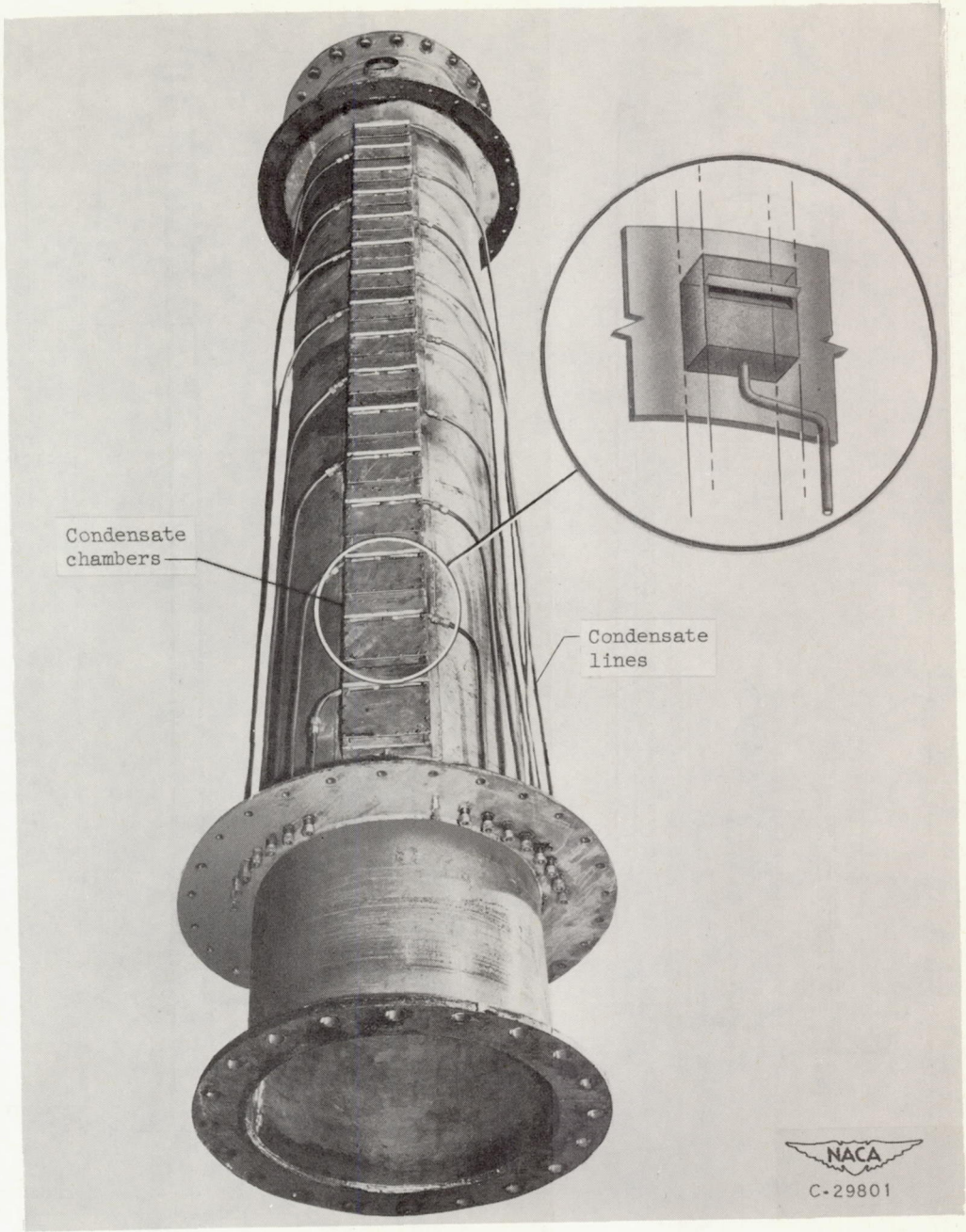

b) Tube with steam jacket removed showing condensate chambers and condensate flow lines.

Figure 1. - Concluded. Mixed-free- and -forced-convection tube.

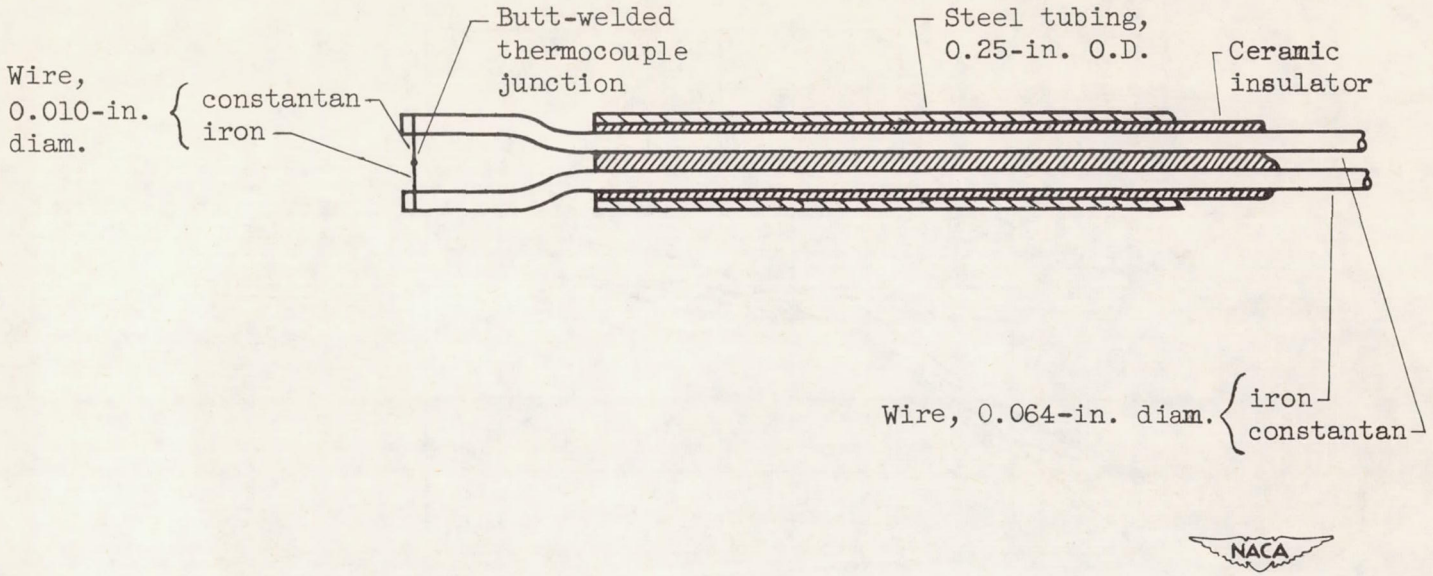

Figure 2. - Iron-constantan thermocouple probe for air-temperature measurement.

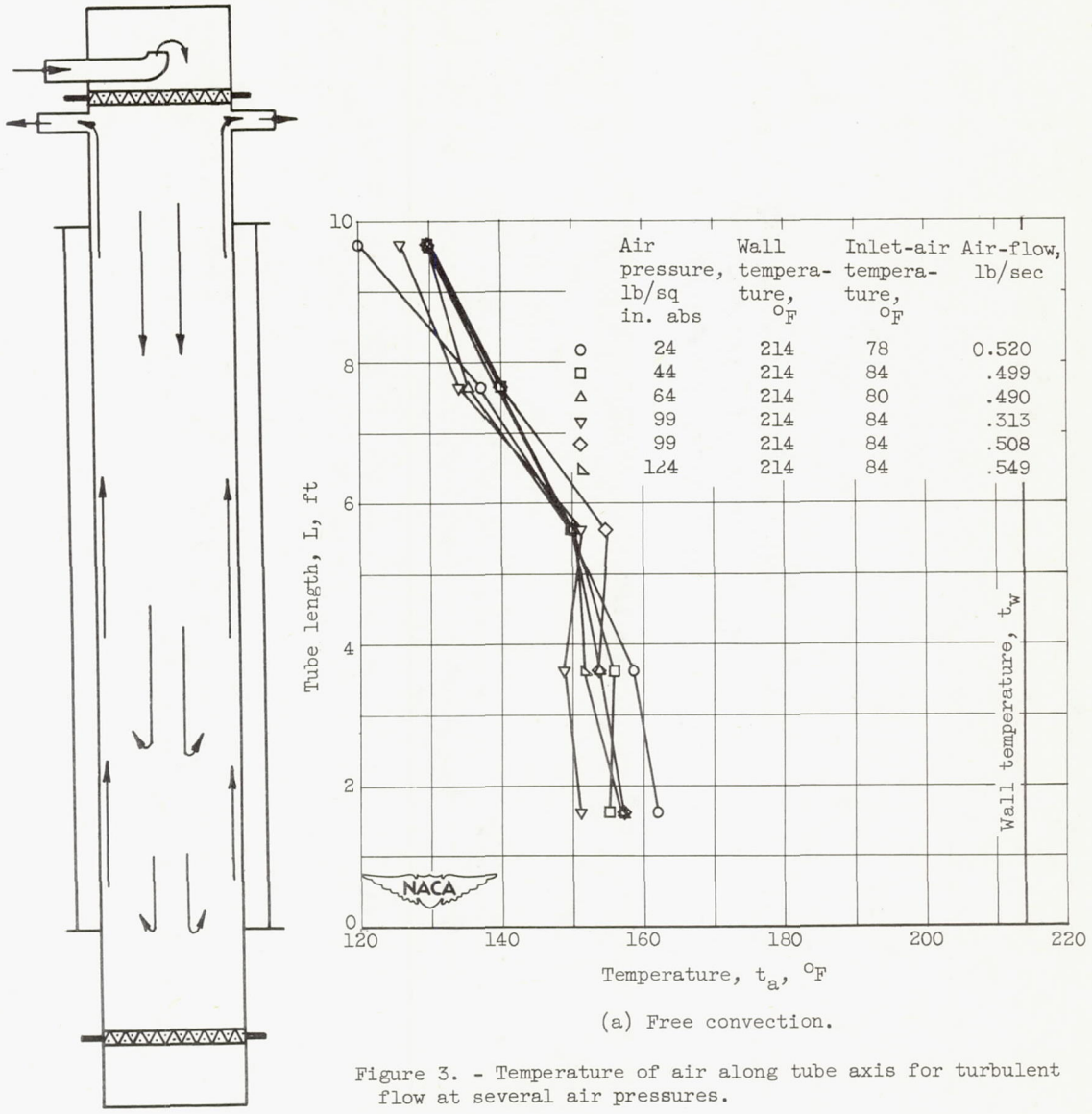

(a) Free convection.

Figure 3. - Temperature of air along tube axis for turbulent flow at several air pressures.

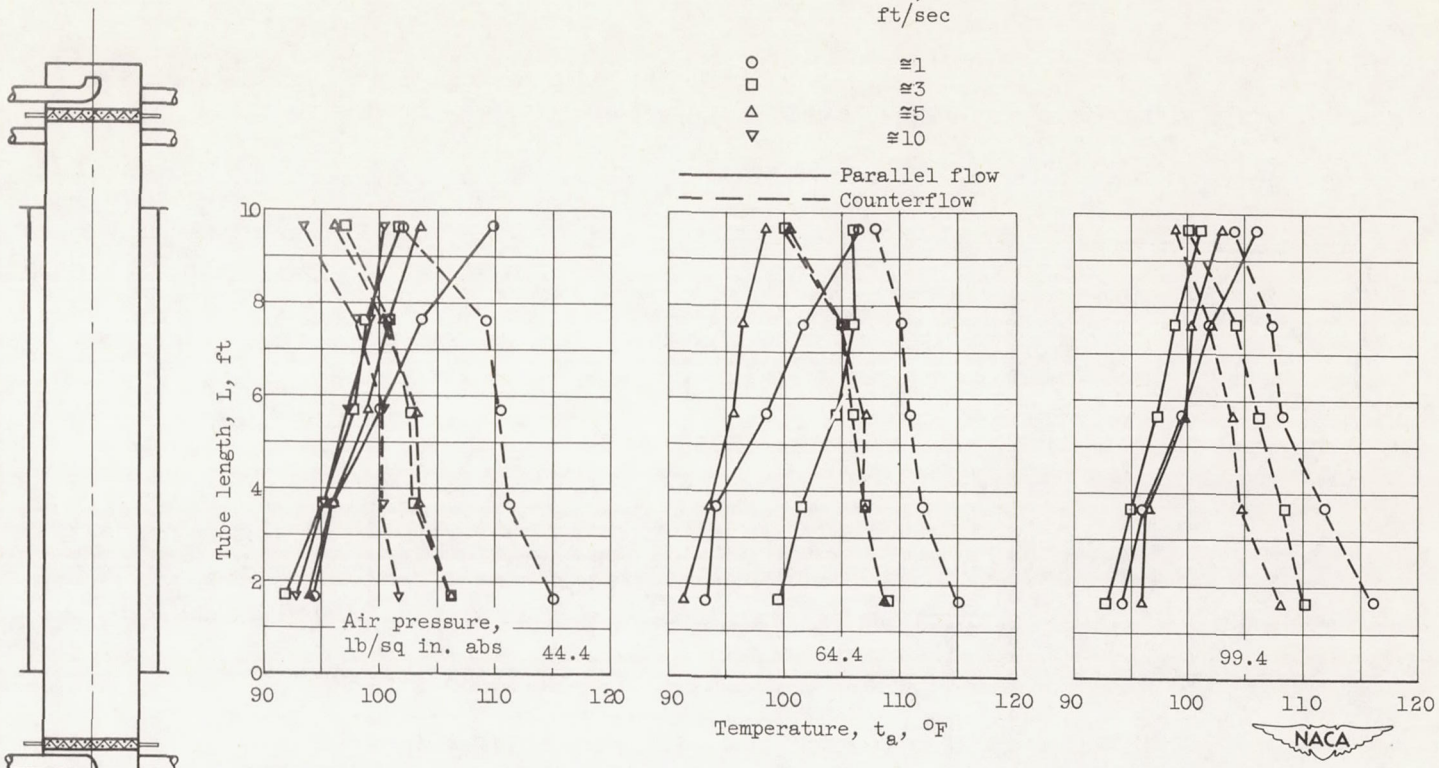

(b) Mixed free and forced convection. Average inlet-air temperature, 86 °F; wall temperature t_w, 217° F (average for all runs).

Figure 3. - Concluded. Temperature of air along tube axis for turbulent flow at several air pressures.

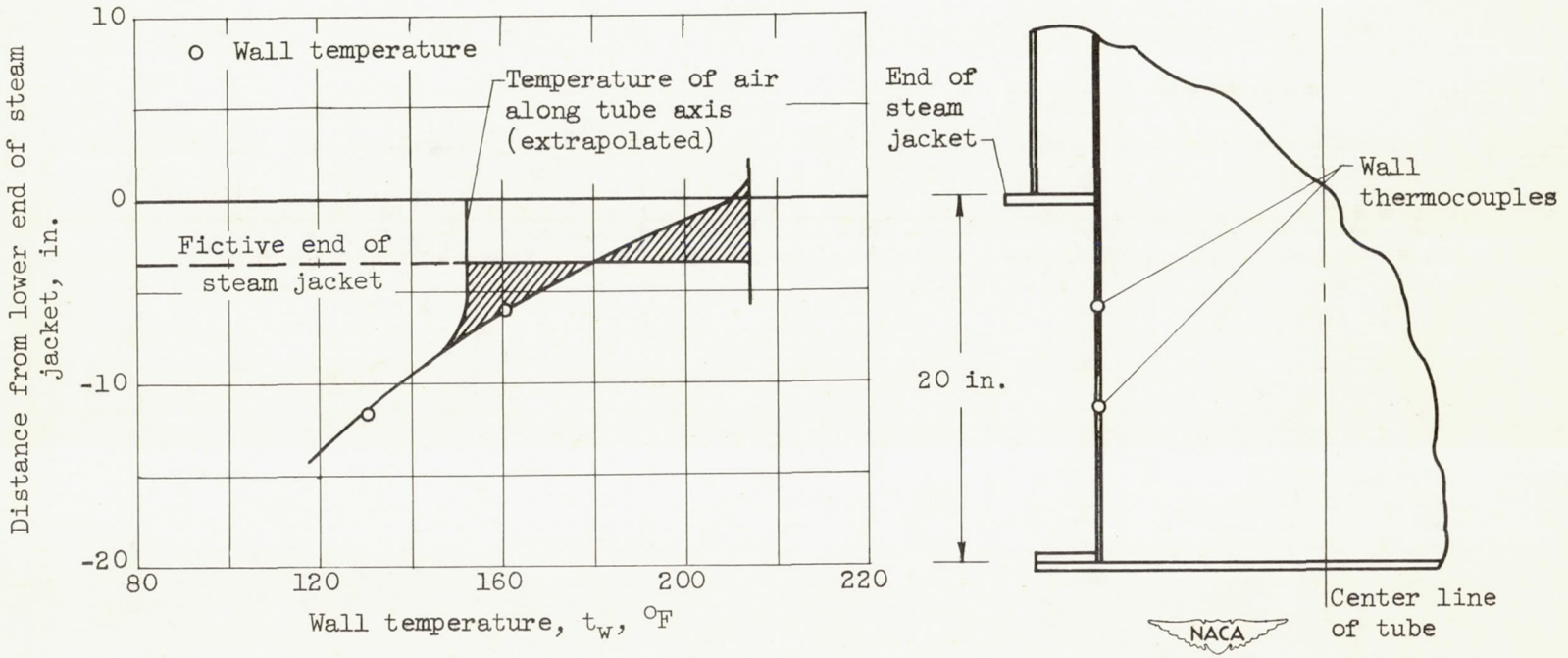

Figure 4. - Determination of fictive lower end of steam jacket for comparison of local heat-transfer data with flat-plate values.

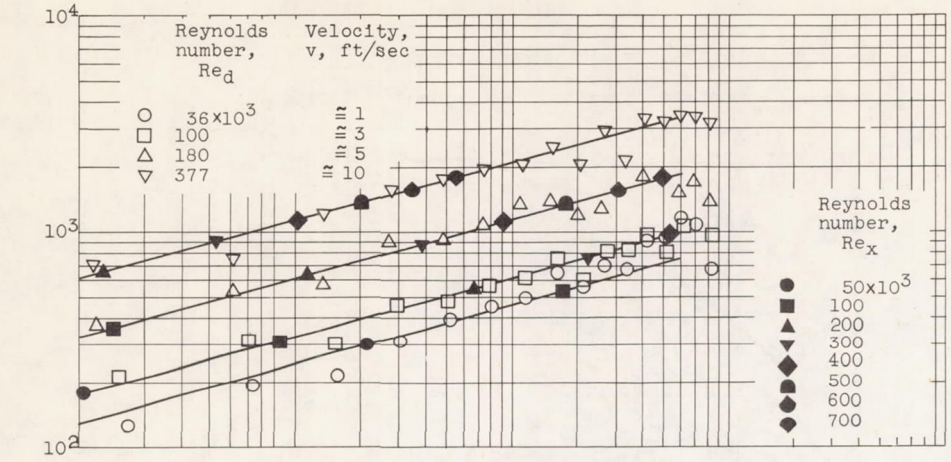

(a) Air pressure, 44.3 pounds per square inch absolute.

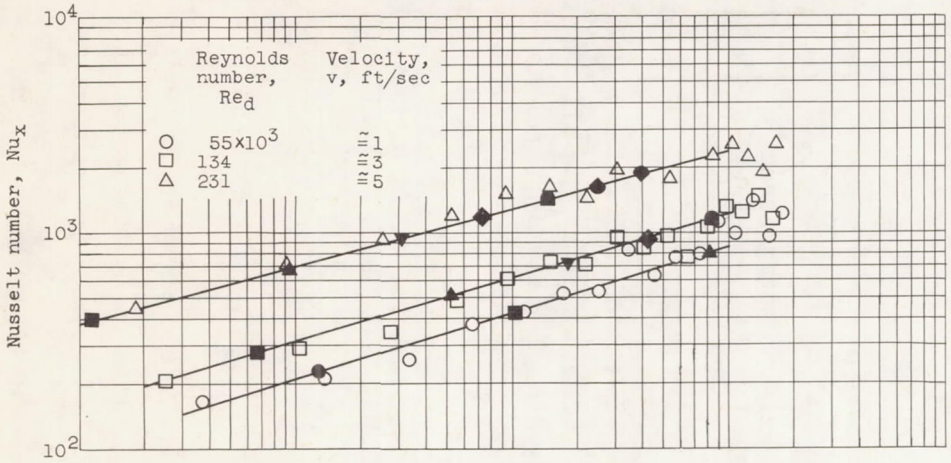

(b) Air pressure, 64.3 pounds per square inch absolute.

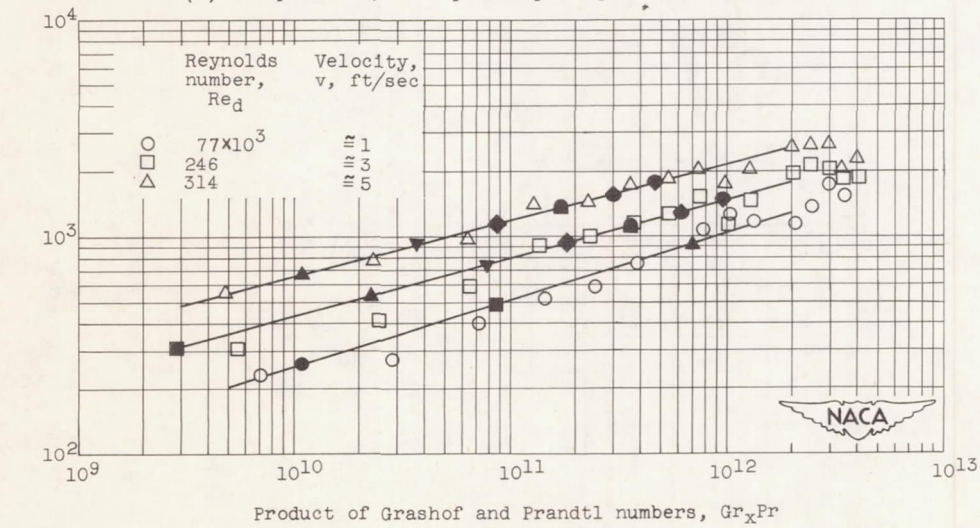

Nusselt number, Nu_x

Product of Grashof and Prandtl numbers, Gr_xPr

(c) Air pressure, 99.3 pounds per square inch absolute.

Figure 5. - Dimensionless correlation of local heat-transfer coefficients for turbulent parallel flow at several air pressures.

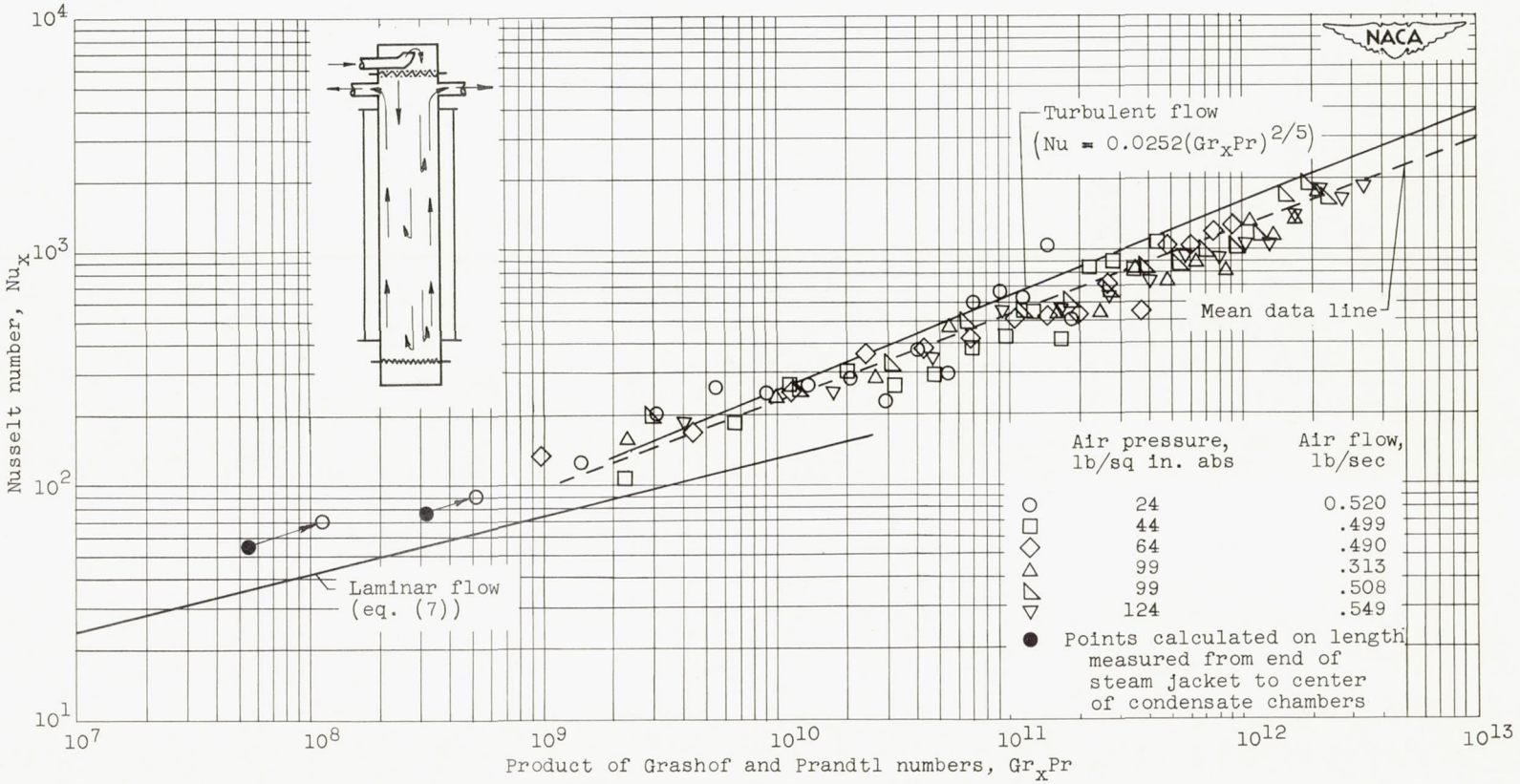

Figure 6. - Dimensionless correlation of local heat-transfer coefficients for turbulent free-convection flow and comparison with known equations for vertical flat plate.

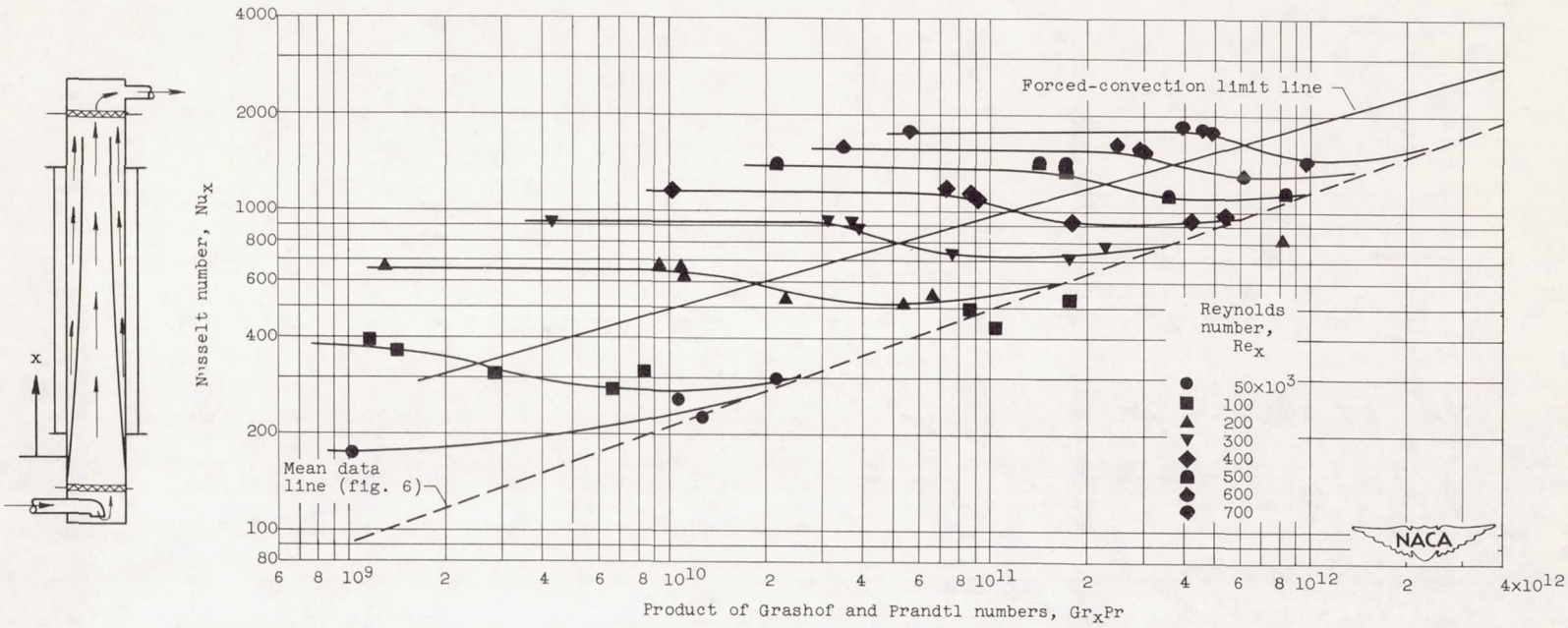

Figure 7. - Dimensionless correlation of local mixed-free- and -forced-convection heat-transfer coefficients for turbulent parallel flow.

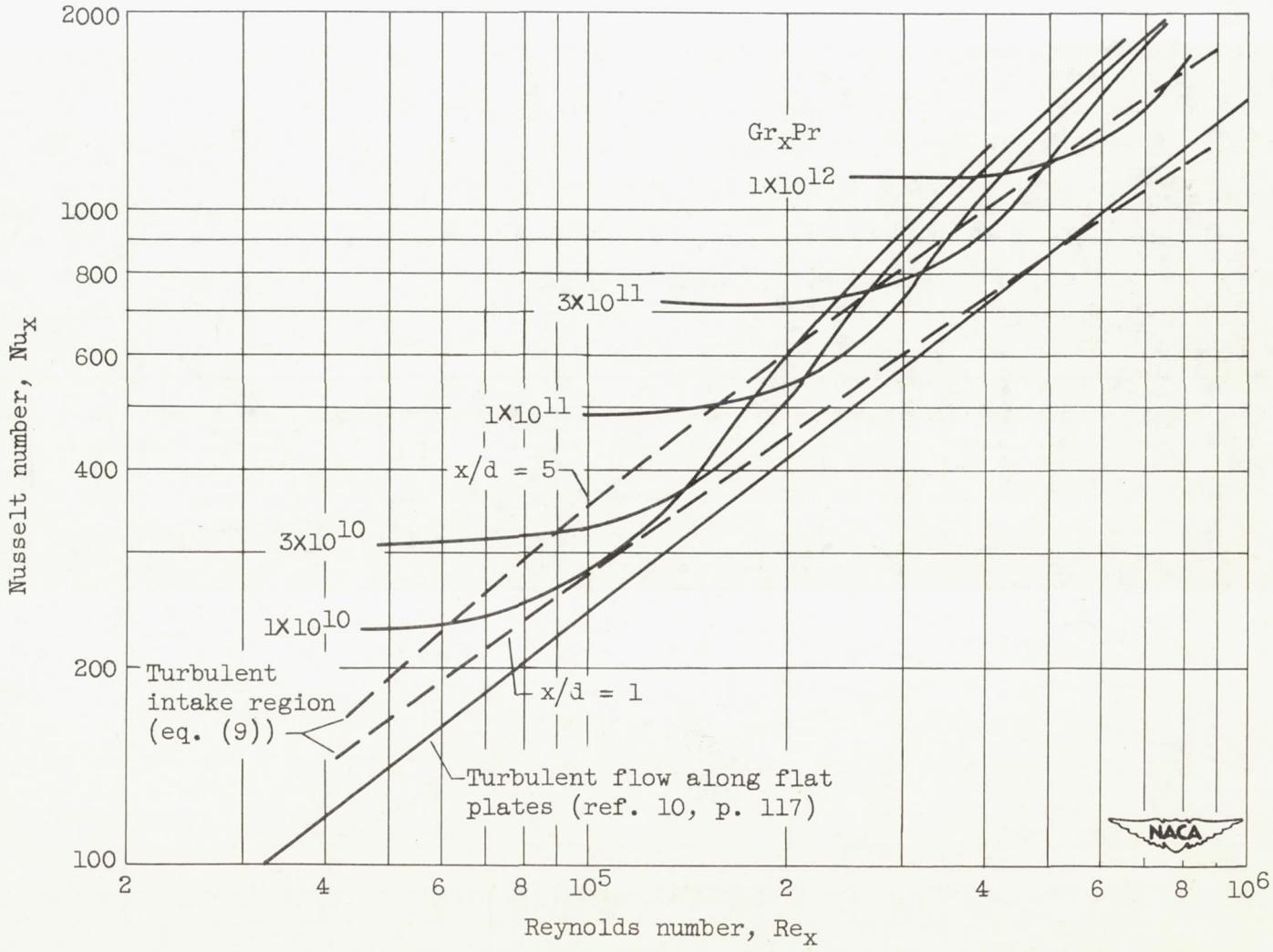

Figure 8. - Dimensionless correlation of mixed-free- and -forced-convection heat-transfer coefficients for turbulent parallel flow.

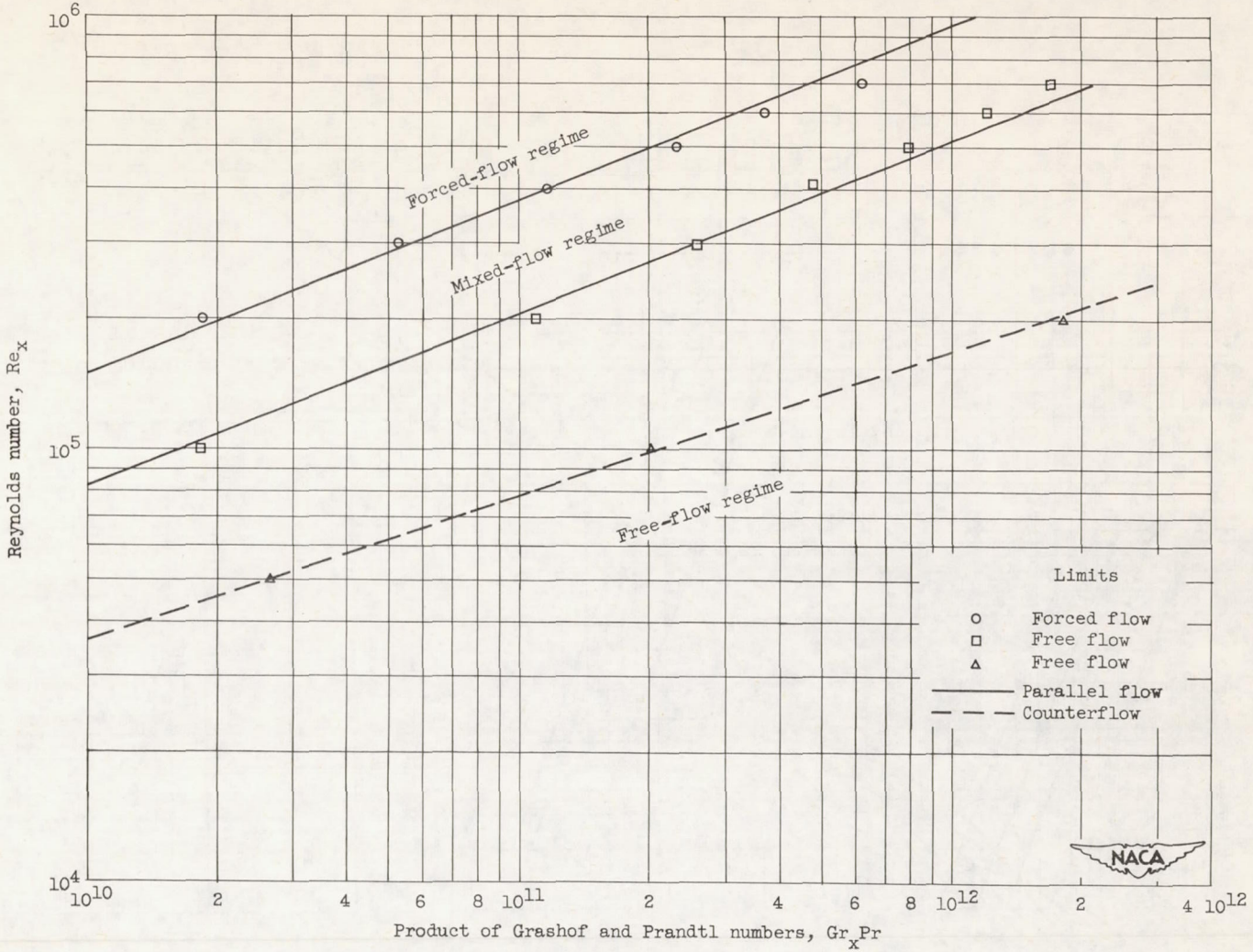

Figure 9. - Free- and forced-convection limits for turbulent flow in tube with length-to-diameter ratio of 5 and Prandtl number of 0.7.

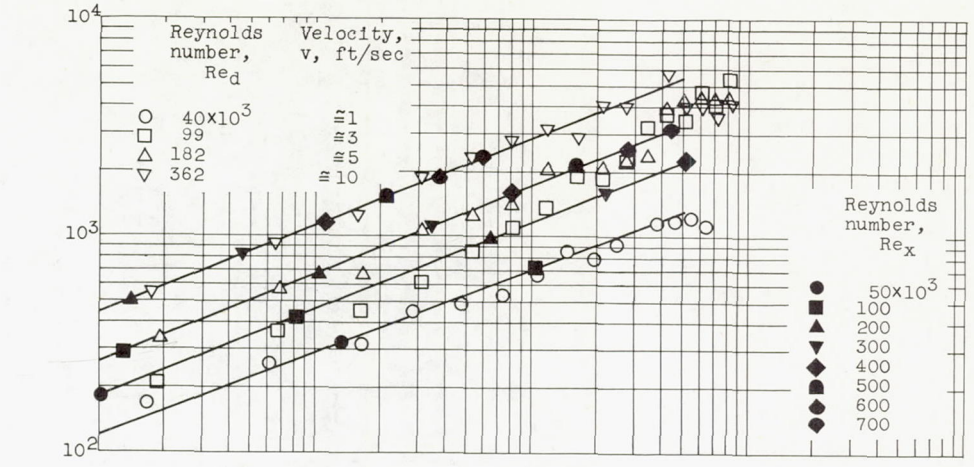

(a) Air pressure, 44.4 pounds per square inch absolute.

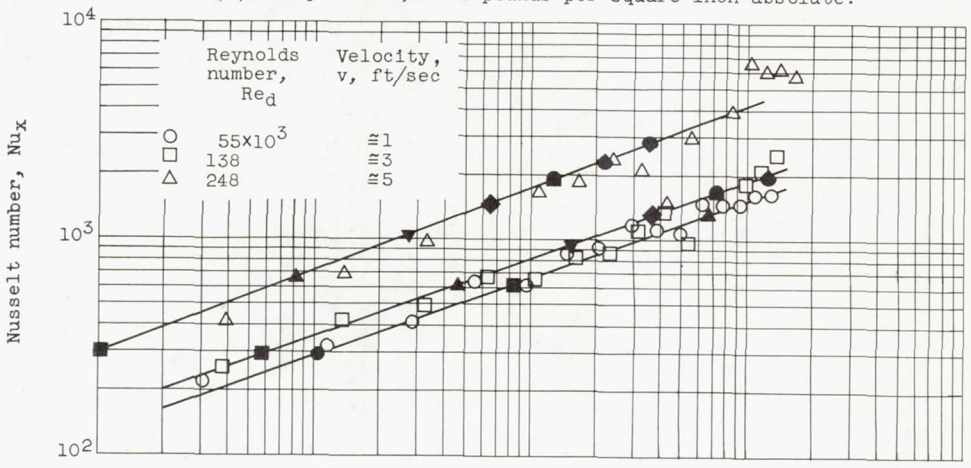

(b) Air pressure, 64.4 pounds per square inch absolute.

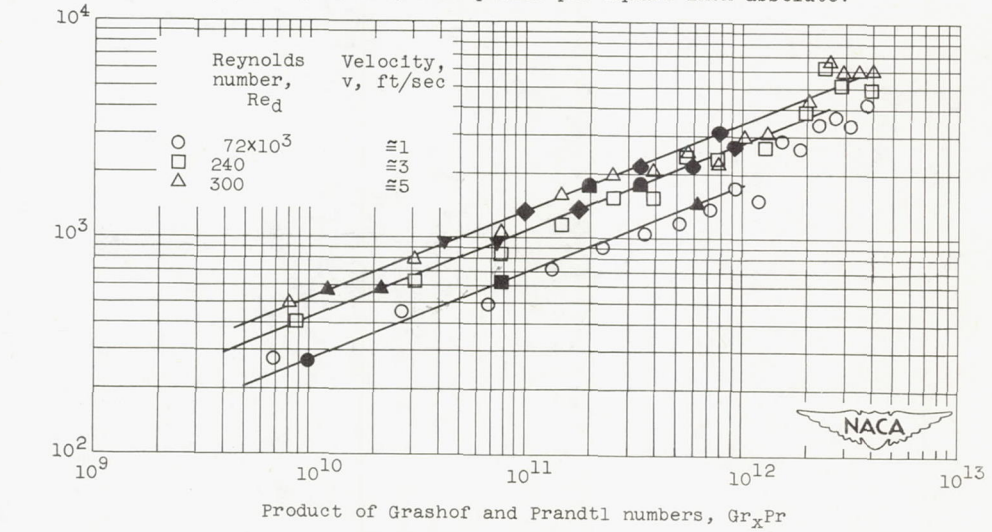

Nusselt number, Nu_x

(c) Air pressure, 99.4 pounds per square inch absolute.

Figure 10. - Dimensionless correlation of local heat-transfer coefficients for turbulent counterflow at several air pressures.

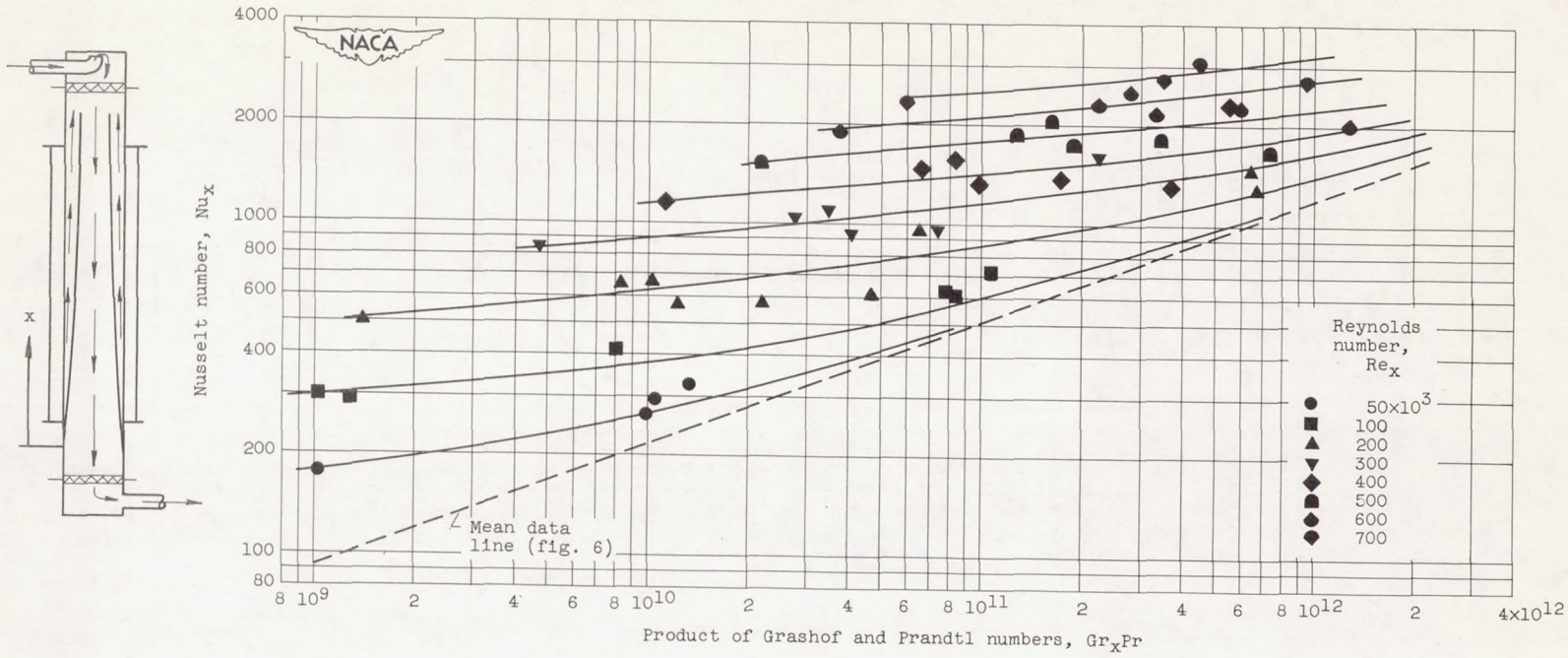

Figure 11. - Dimensionless correlation of local mixed-free- and -forced-convection heat-transfer coefficients for turbulent counterflow.

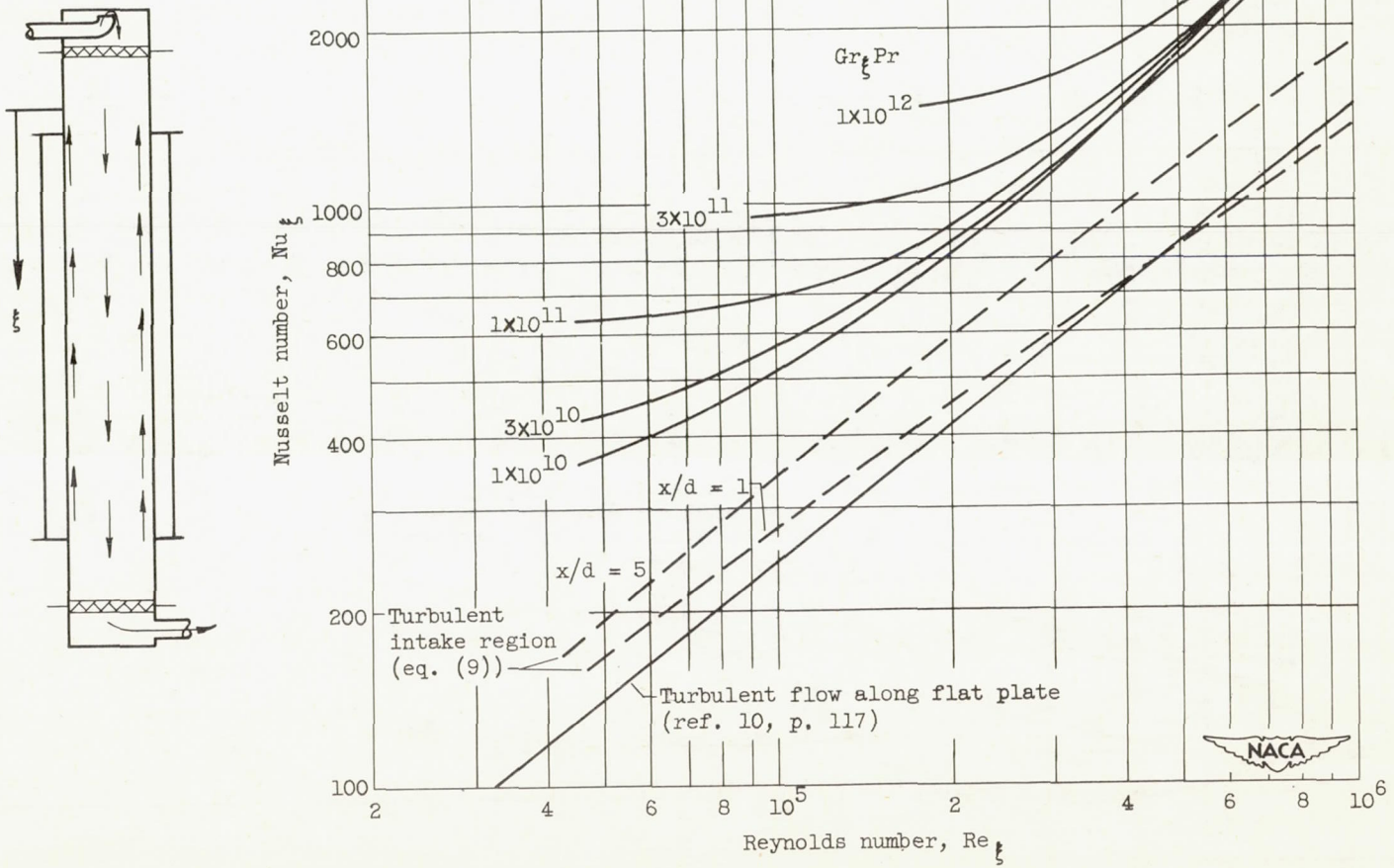

Figure 12. - Dimensionless correlation of mixed-free- and -forced-convection heat-transfer coefficients for turbulent counterflow.

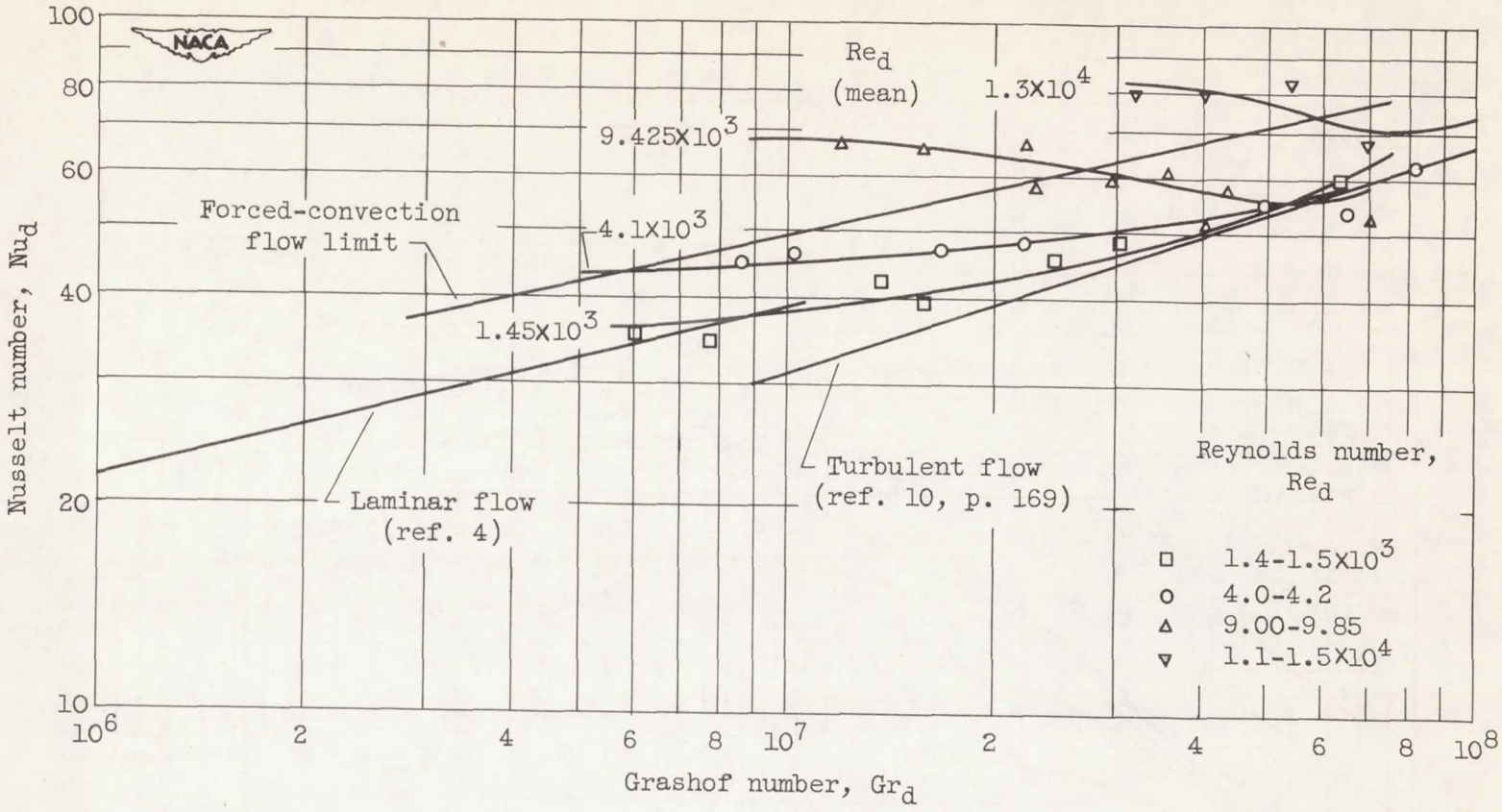

Figure 13. - Dimensionless correlation of experimental heat-transfer data in vertical tube (length-to-diameter ratio, 20; Prandtl number, approximately 3.0) obtained by Watzinger and Johnson (ref. 4).

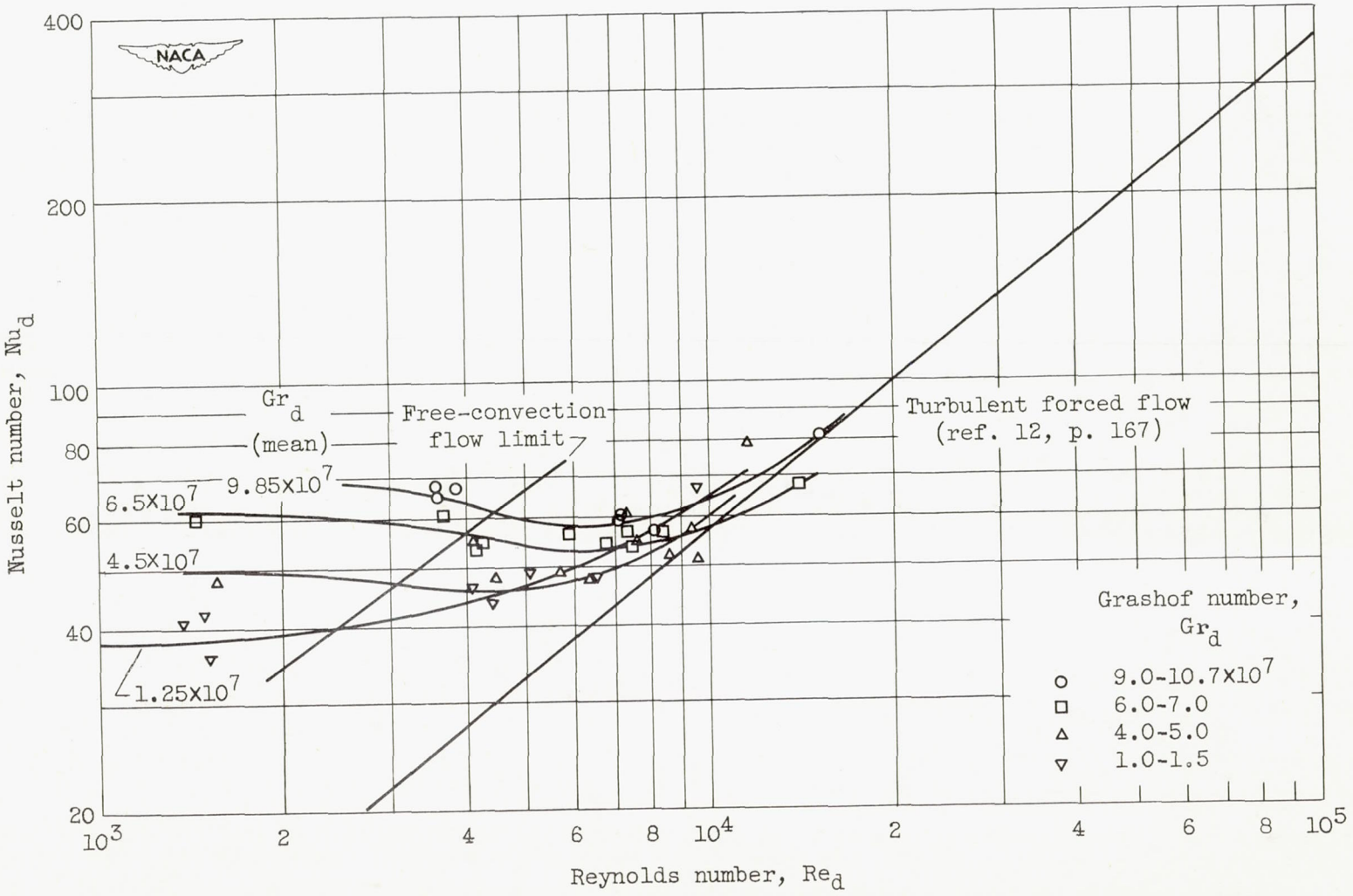

Figure 14. - Dimensionless correlation of experimental heat-transfer data in vertical tube (length-to-diameter ratio, 20; Prandtl number, approximately 3.0) obtained by Watzinger and Johnson (ref. 4).

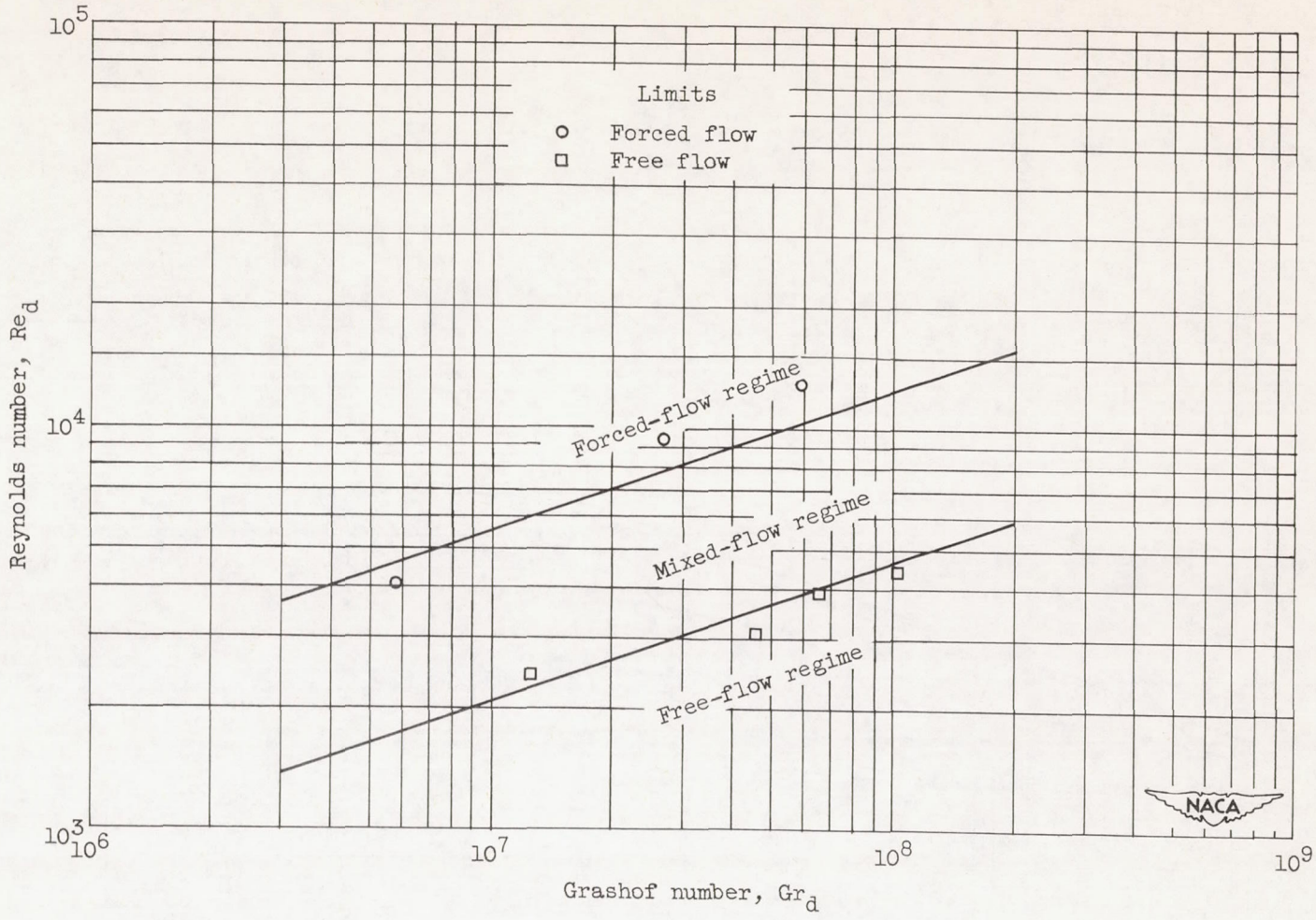

Figure 15. - Free- and forced-convection limits for experimental results obtained by Watzinger and Johnson (ref. 4). Length-to-diameter ratio of tube, 20; Prandtl number, approximately 3.0.

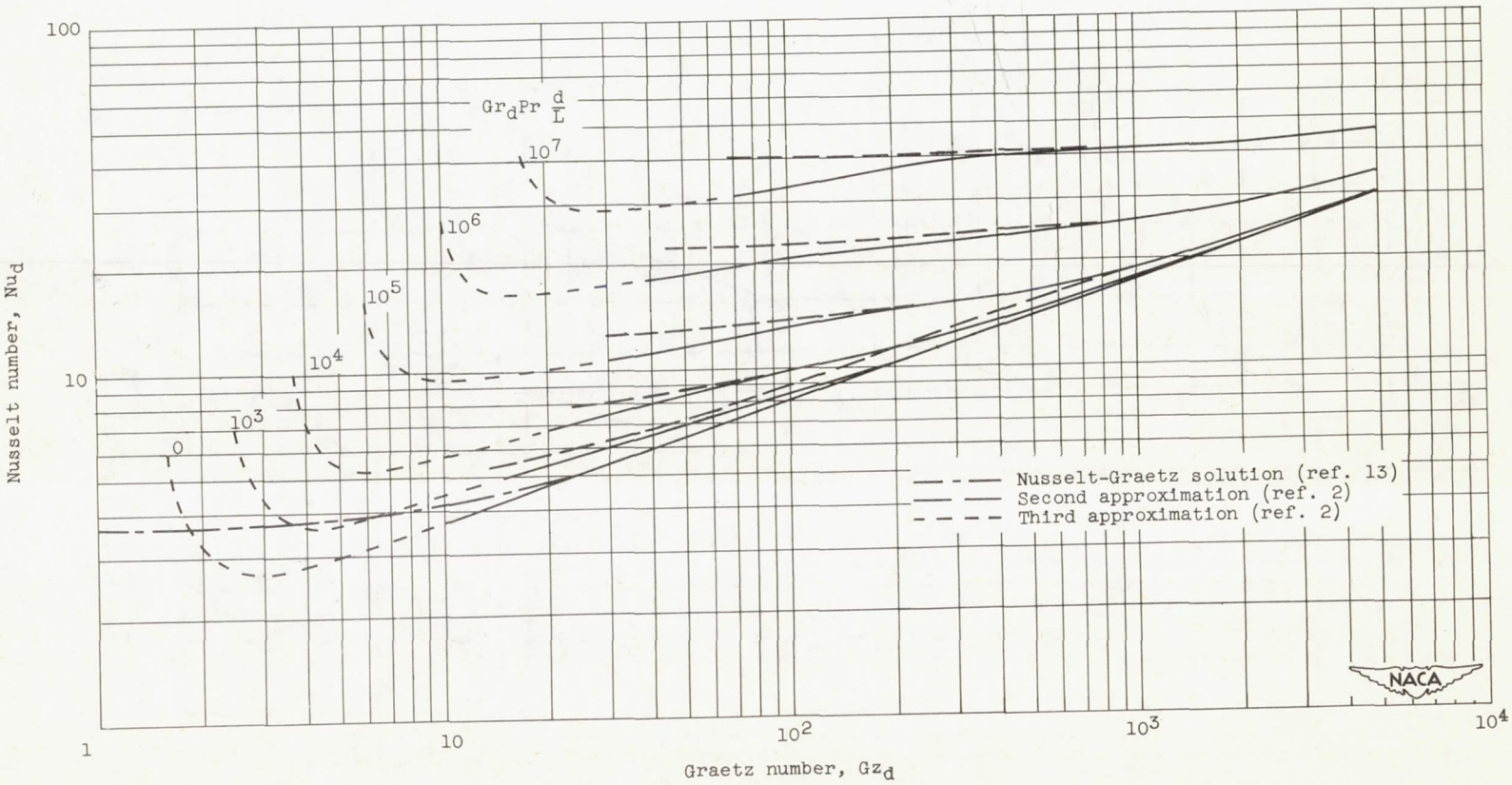

Figure 16. - Dimensionless correlation of mixed-free- and -forced-convection heat-transfer coefficients for laminar flow in vertical tube as predicted by Martinelli and Boelter (ref. 2).

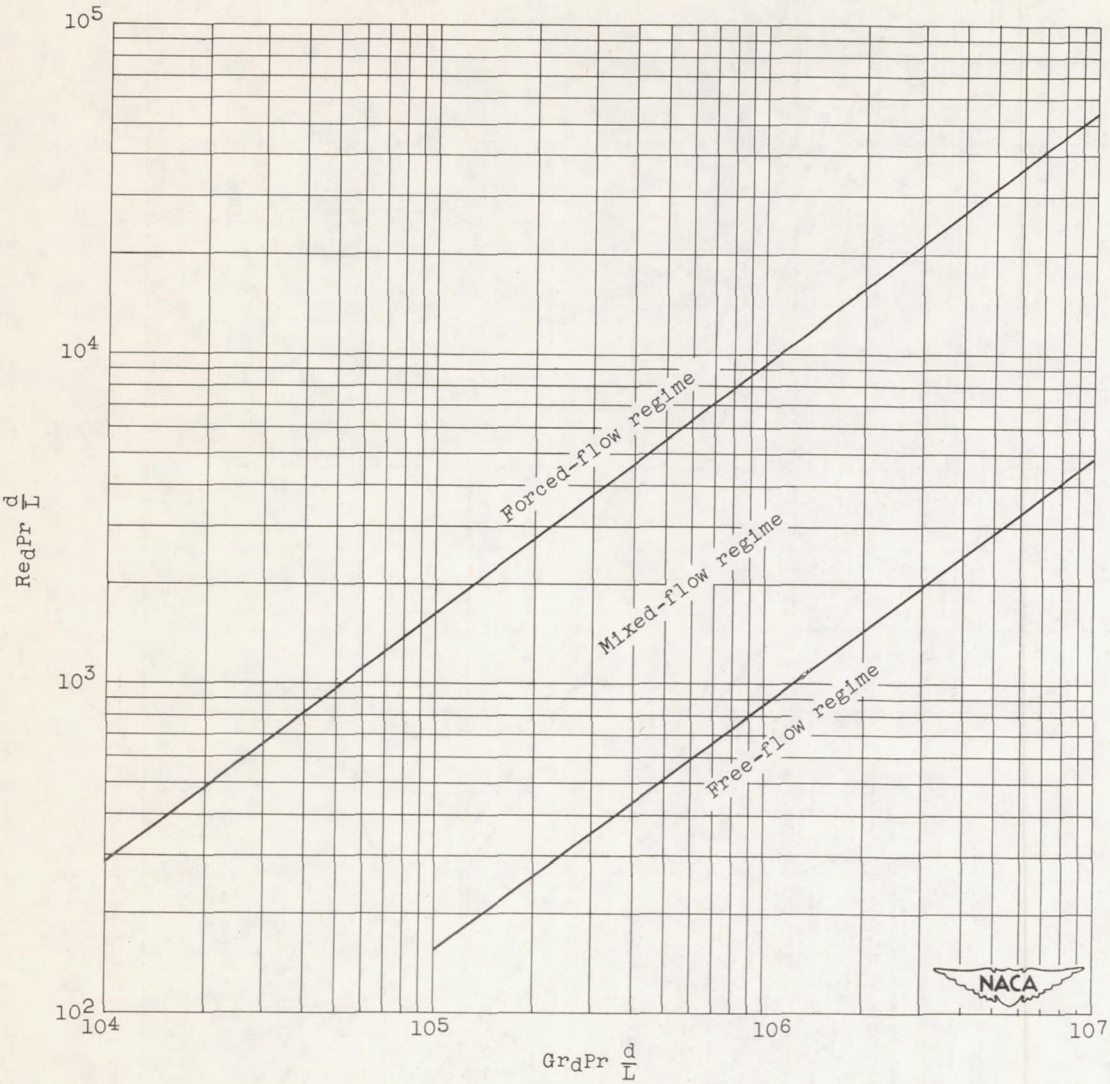

Figure 17. - Free- and forced-convection limits for laminar flow as determined from Martinelli and Boelter analysis (ref. 2).

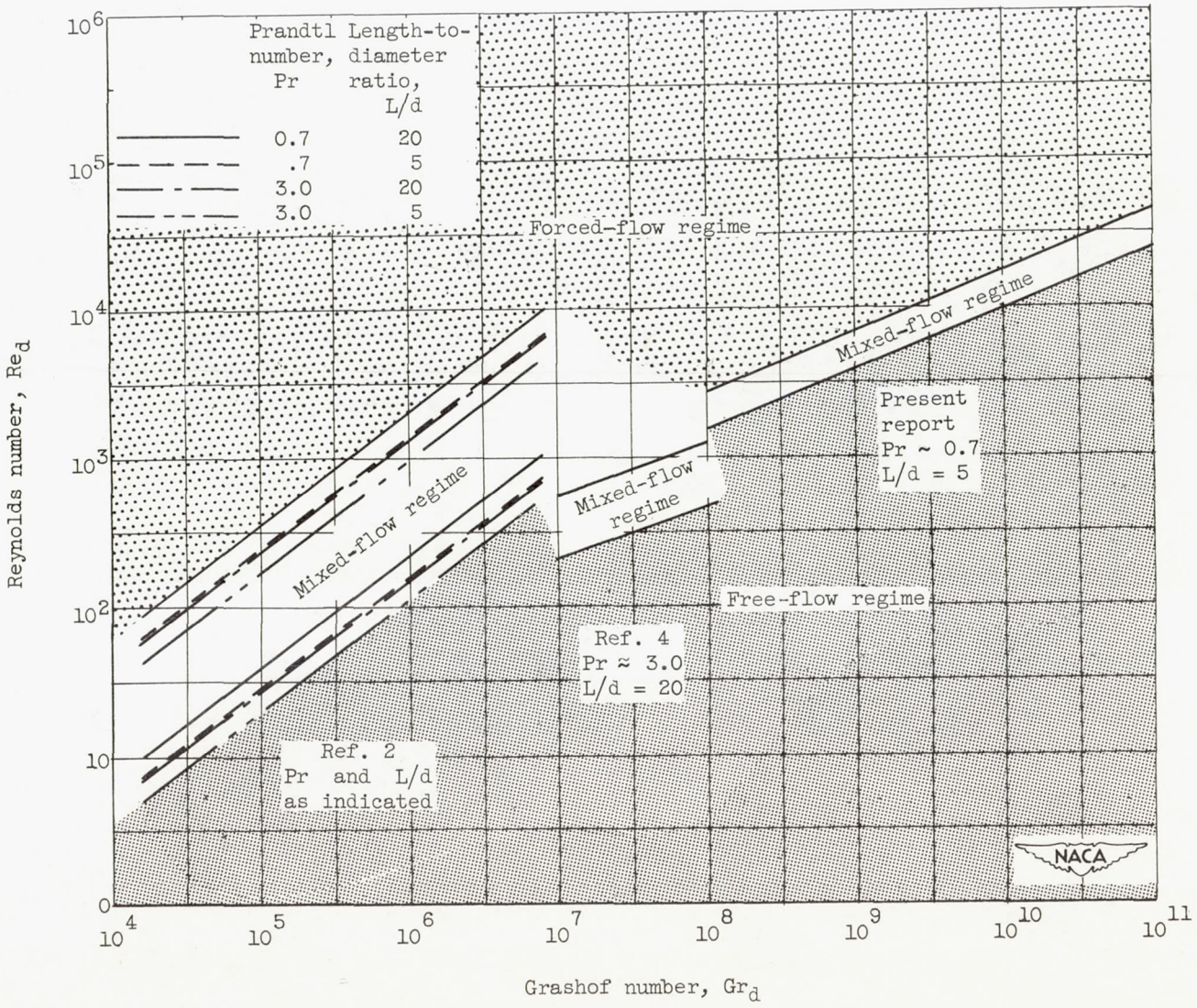

Figure 18. - Summary of available data on free-, forced-, and mixed-flow regimes in parallel flow.

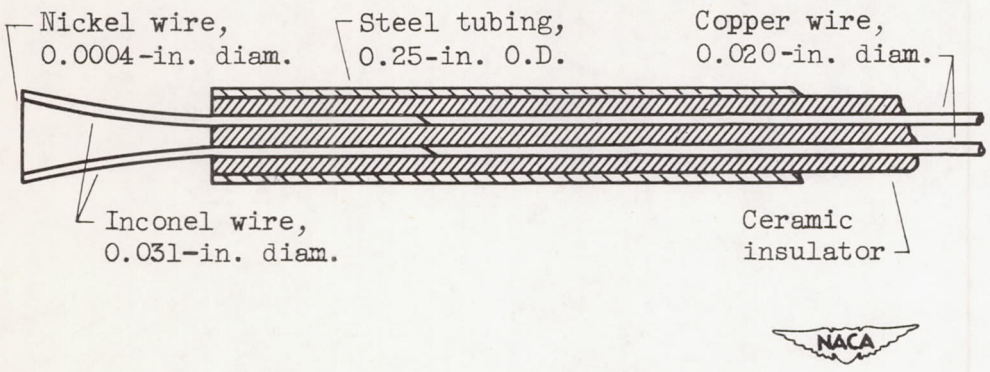

Figure 19. - Hot-wire instrument probe for air-temperature and velocity surveys.

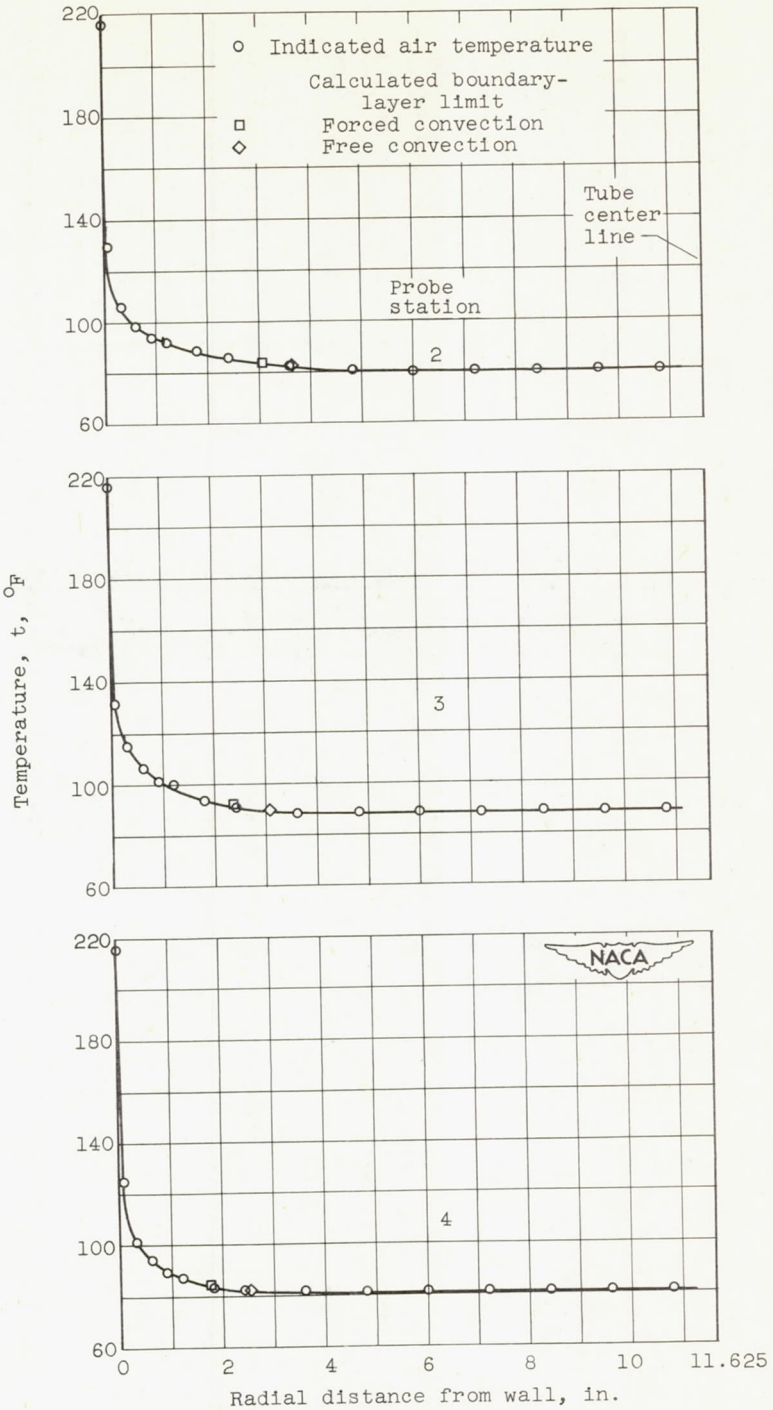

(a) Velocity, approximately 1 foot per second.

Figure 20. - Turbulent-air-temperature profiles measured by a hot-wire instrument along tube radius at three probe stations for parallel flow. Air pressure, 64.3 pounds per square inch absolute.

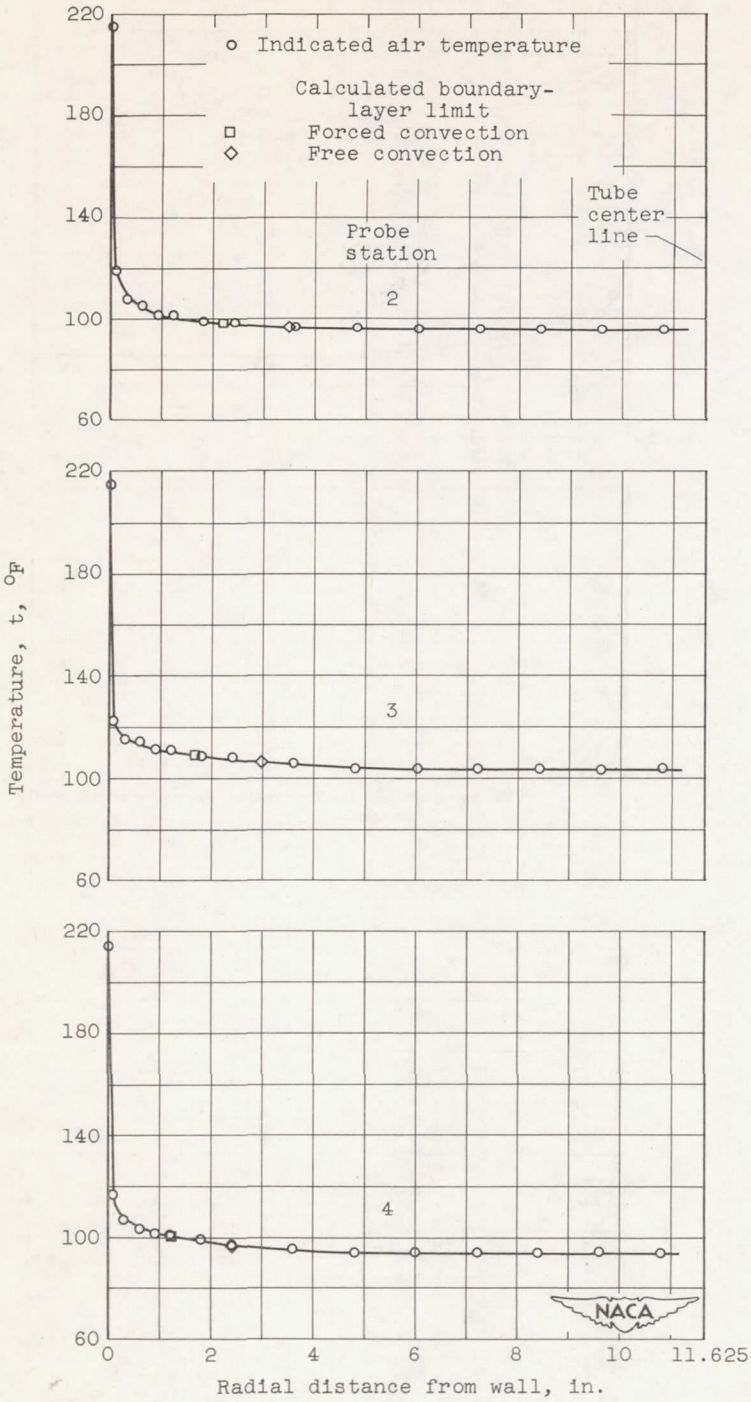

(b) Velocity, approximately 5 feet per second.

Figure 20. - Concluded. Turbulent-air-temperature profiles measured by a hot-wire instrument along tube radius at three probe stations for parallel flow. Air pressure, 64.3 pounds per square inch absolute.

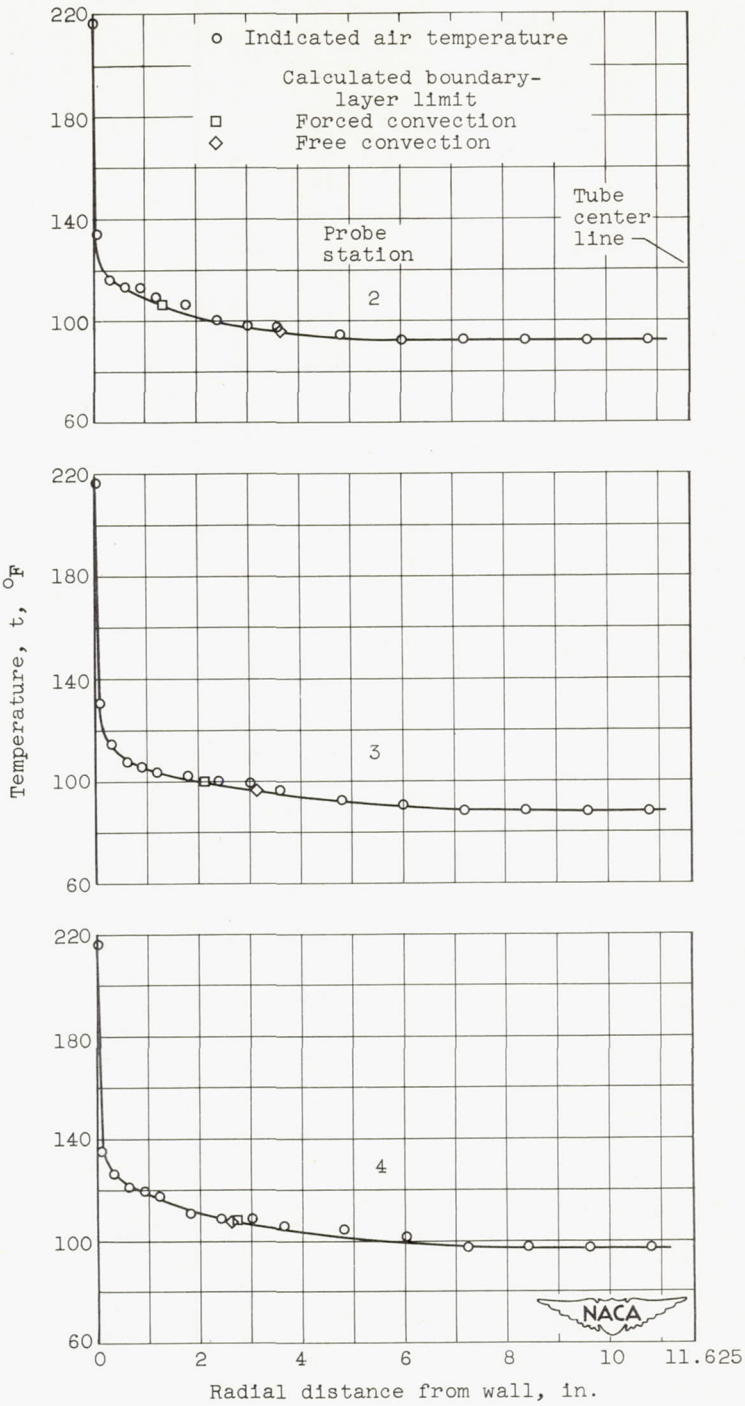

(a) Velocity, approximately 1 foot per second.

Figure 21. - Turbulent-air-temperature profiles measured by a hot-wire instrument along tube radius at three probe stations for counterflow. Air pressure, 64.4 pounds per square inch absolute.

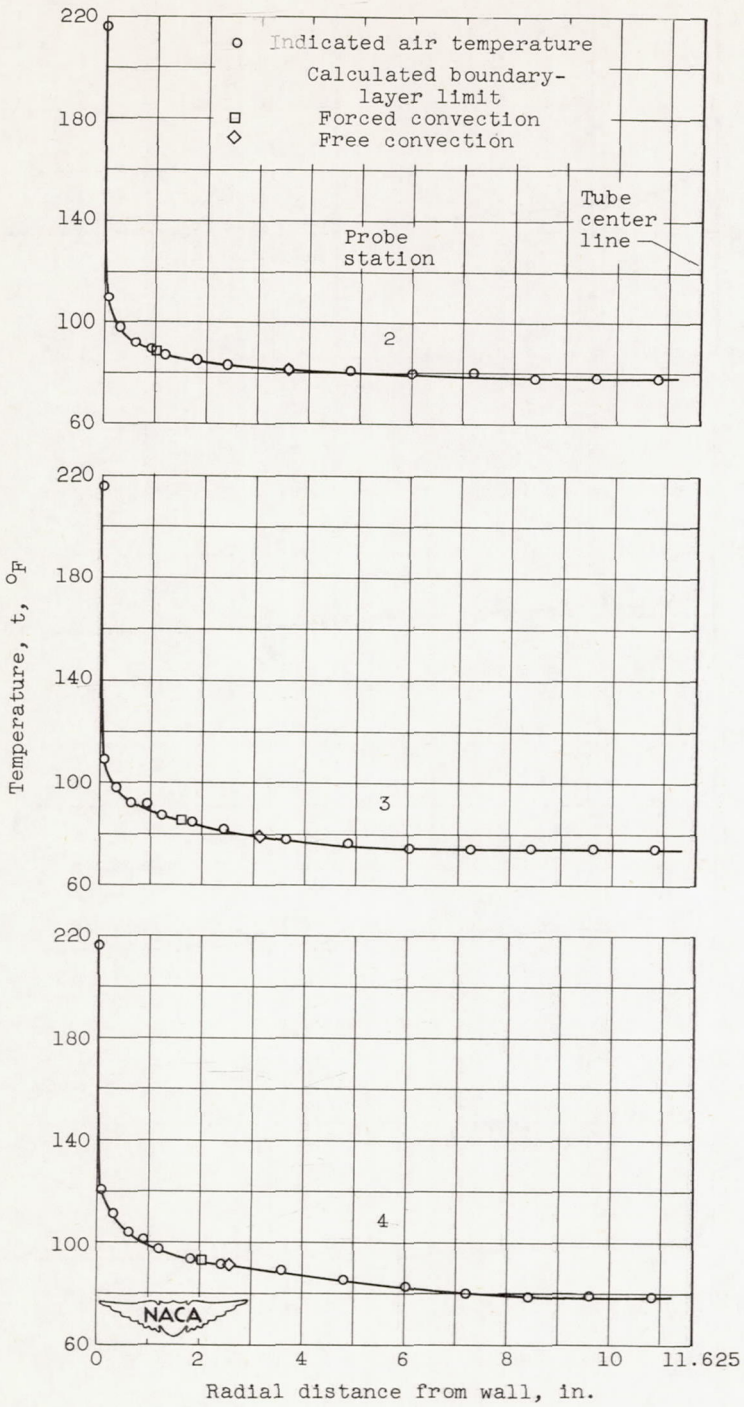

(b) Velocity, approximately 5 feet per second.

Figure 21. - Concluded. Turbulent-air-temperature profiles measured by a hot-wire instrument along tube radius at three probe stations for counterflow. Air pressure, 64.4 pounds per square inch absolute.

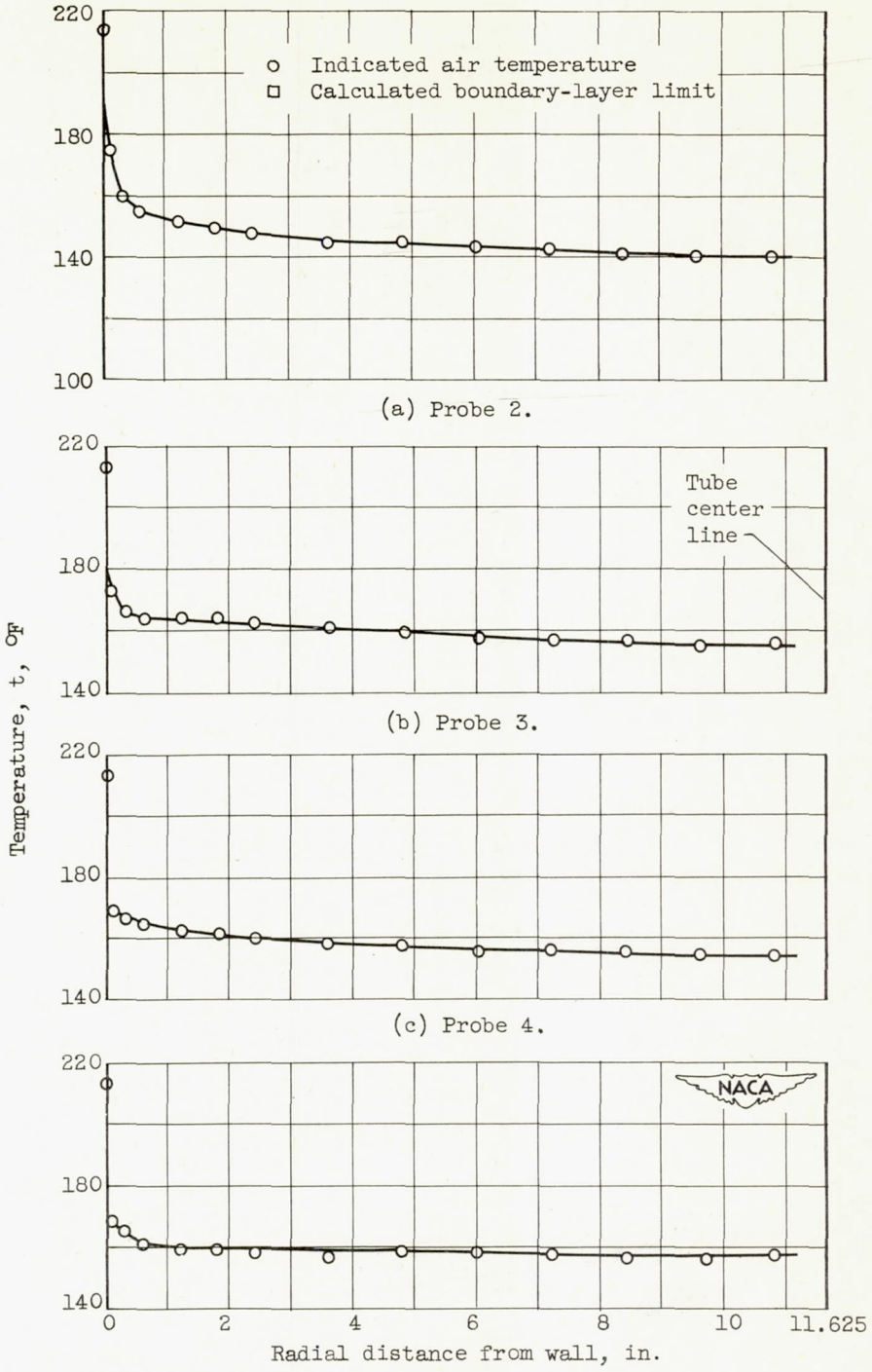

Figure 22. - Turbulent-air-temperature profiles measured by thermocouples at four probe locations along axis for free-convection flow. Air pressure, 99 pounds per square inch absolute; air flow, 0.313 pound per second.

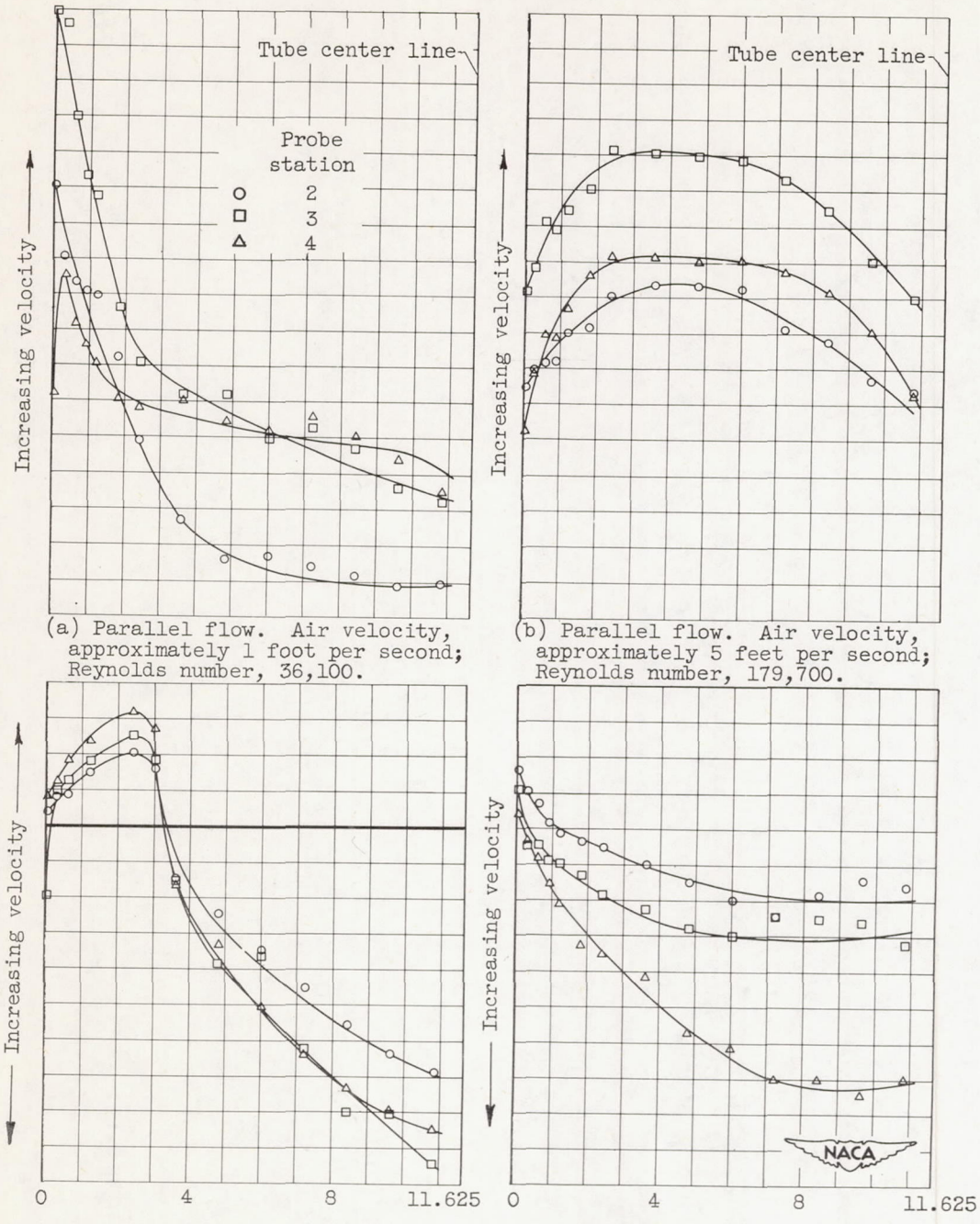

(a) Parallel flow. Air velocity, approximately 1 foot per second; Reynolds number, 36,100.

(b) Parallel flow. Air velocity, approximately 5 feet per second; Reynolds number, 179,700.

(c) Counterflow. Air velocity, approximately 1 foot per second; Reynolds number, 40,500.

(d) Counterflow. Air velocity, approximately 5 feet per second; Reynolds number, 182,500.

Figure 23. - Air-velocity profiles along tube radius at several probe stations. Air pressure, 64.4 pounds per square inch absolute.